Drastic Vegetation Change in the Guajira Peninsula (Colombia) During the Neogene

Carlos Jaramillo, Pierre Sepulchre, Damian Cardenas, Alexander Correa-metrio, J. Enrique Moreno, Raul Trejos, Diego Vallejos, Natalia Hoyos, Camila Martínez, Daniella Carvalho, et al.

Paleoceanography and Paleoclimatology

RESEARCH ARTICLE
10.1029/2020PA003933

Special Section:
The Miocene: The Future of the Past

Drastic Vegetation Change in the Guajira Peninsula (Colombia) During the Neogene

Carlos Jaramillo[1,2,3], Pierre Sepulchre[4], Damian Cardenas[1,5], Alexander Correa-Metrio[6], J. Enrique Moreno[1], Raul Trejos[7], Diego Vallejos[7], Natalia Hoyos[8], Camila Martínez[1], Daniella Carvalho[1], Jaime Escobar[1,8], Francisca Oboh-Ikuenobe[5], Mercedes B. Prámparo[9], and Diego Pinzón[9]

[1]Smithsonian Tropical Research Institute, Panamá City, Panamá, [2]ISEM, U. Montpellier, CNRS, EPHE, IRD, Montpellier, France, [3]Department of Geology, Faculty of Sciences, University of Salamanca, Salamanca, Spain, [4]Laboratoire des Sciences du Climat et de l'Environnement, LSCE/IPSL, CEA-CNRS-UVSQ, Université Paris-Saclay, Gif-sur-Yvette, France, [5]Department of Geosciences and Geological and Petroleum Engineering, Missouri University of Science and Technology, Rolla, MO, USA, [6]Instituto de Geología, Universidad Nacional Autónoma de México, Mexico City, Mexico, [7]Department of Geology, Universidad de Caldas, Manizales, Colombia, [8]Universidad del Norte, Barranquilla, Colombia, [9]IANIGLA, CCT-CONICET, Mendoza, Argentina

Key Points:
- The Guajira Peninsula had a high mean annual precipitation during the early Miocene, which supported a tropical rainforest biome
- This setting constrasts sharply with the modern dry climate, which supports a xerophytic biome
- Miocene climate simulations do not reproduce high rainfall for this region. Mechanisms driving this change are still to be determined

Supporting Information:
- Supporting Information S1

Correspondence to:
C. Jaramillo,
jaramilloc@si.edu

Citation:
Jaramillo, C., Sepulchre, P., Cardenas, D., Correa-Metrio, A., Moreno, J. E., Trejos, R., et al. (2020). Drastic vegetation change in the Guajira Peninsula (Colombia) during the Neogene. *Paleoceanography and Paleoclimatology*, *35*, e2020PA003933. https://doi.org/10.1029/2020PA003933

Received 27 MAR 2020
Accepted 14 OCT 2020
Accepted article online 16 OCT 2020

Abstract Dry biomes occupy ~35% of the landscape in the Neotropics, but these are heavily human-disturbed. In spite of their importance, we still do not fully understand their origins and how they are sustained. The Guajira Peninsula in northern Colombia is dominated by dry biomes and has a rich Neogene fossil record. Here, we have analyzed its changes in vegetation and precipitation during the Neogene using a fossil pollen and spore dataset of 20 samples taken from a well and we also dated the stratigraphic sequence using microfossils. In addition, we analyzed the pollen and spore contents of 10 Holocene samples to establish a modern baseline for comparison with the Neogene as well as a study of the modern vegetation to assess both its spatial distribution and anthropic disturbances during the initial stages of European colonization. The section was dated to span from the latest Oligocene to the early Miocene (~24.2 to 17.3 Ma), with the Oligocene/Miocene boundary being in the lower Uitpa Formation. The early Miocene vegetation is dominated by a rainforest biome with a mean annual precipitation of ~2,000 mm/yr, which strongly contrasts with Guajira's modern xerophytic vegetation and a precipitation of ~300 mm/yr. The shift to the dry modern vegetation probably occurred over the past three millions years, but the mechanism that led to this change is still uncertain. Global circulation models that include the vegetation could explain the ancient climate of Guajira, but further work is required to assess the feedbacks of vegetation, precipitation, and CO_2.

1. Introduction

Among the diverse array of biomes in the Neotropics are dry ecosystems such as tropical savannas, Cerrado, Caatinga, and both dry and xerophytic forests. These dry settings, which occupy ~35% of the total area (Azevedo et al., 2020), also support a population of more than 40 million people and thus have been heavily disturbed by human habitation and food production. Despite their geographic extent and societal importance, we still know little about their origins and what sustains them through time. How long have they been present? What factors drove their geographic expansion and biotic diversification? How do the climate and the biota interact in these ecosystems?

The northern-most region of South America, including the Guajira Peninsula in Colombia, is characterized by an arid climate and a landscape dominated by xerophytic vegetation (Figure 1). Cacti and the legume *Prosopis* are some of the dominant plants in the landscape (Figure 2). The dry climate has created excellent exposures of the Neogene sequence in the Guajira's Cocinetas Basin, which have spawned numerous stratigraphic and paleontological studies over the past decade. During the middle Miocene to early Pliocene, the fossil record of crocodiles, turtles, fishes, and mammals suggests the presence of permanent and widespread bodies of water, including both rivers and lakes (Aguilera et al., 2013; Amson et al., 2016; Cadena & Jaramillo, 2015a, 2015b; Carrillo et al., 2018; Florez et al., 2018a, 2018b; Forasiepi et al., 2014; Jaramillo et al., 2015; Moreno et al., 2015; Moreno-Bernal et al., 2016; Perez et al., 2017; Suarez

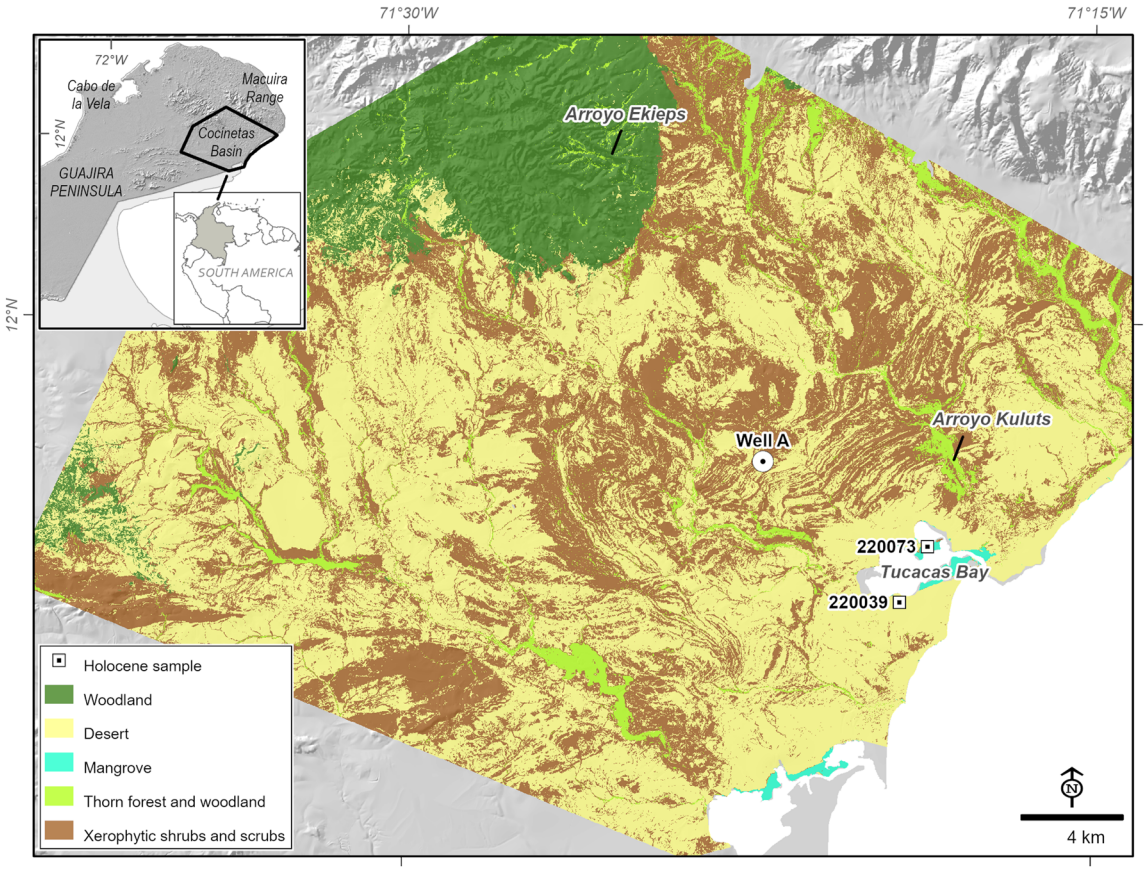

Figure 1. Modern ecosystem map for the Cocinetas Basin. For a description of each ecosystem type, refer to Table 1. Data sources listed in Table S2. The location of Well A and the sites where surficial sediment samples were collected are also included.

et al., 2016). However, paleobotanical evidence was lacking as previous attempts to find plant macrofossils and pollen/spores in outcropping strata had been unsuccessful. Here, we present the fossil pollen record obtained from ditch-cutting samples from one of only two wells that have been drilled in the basin. The recovery of palynologically productive samples from the well suggests that plant remains in outcrop samples have been degraded by modern weathering rather than being absent during accumulation.

The Cenozoic sequence of the Cocinetas Basin comprises, in ascending order, the Siamana, Uitpa, Jimol, Castilletes, and Ware formations (Moreno et al., 2015), and the studied well only encompassed from the upper Siamana to lower Jimol formations. The ages of the Siamana Formation and the lower part of the Uitpa Formation are poorly constrained. The Siamana Formation, a massive reef unit that was likely part of the extensive reef development in the Caribbean during the late Oligocene (Johnson et al., 2009), has been variously dated as early Miocene, late Oligocene, or both (Carrillo-Briceño et al., 2016; Florez et al., 2018a, 2018b; Silva-Tamayo et al., 2017). In order to solve this age uncertainty, we dated the well sequence by performing a detailed biostratigraphic analysis using calcareous nannoplankton, foraminifera, and palynomorphs (dinoflagellates, pollen, and spores).

The pollen and spore records of the well were analyzed to assess the type of biome present in Guajira during the Neogene and to estimate mean annual precipitation (MAP) and mean annual temperature (MAT). In order to compare the fossil palynological record with the modern vegetation of the region, both the pollen record of surficial samples of modern environments and the spatial distribution of the modern vegetation were analyzed. We also conducted a review of sixteenth century Spanish records to determine, as some have argued, whether the modern vegetation of Guajira could have been a byproduct of the Spanish colonization.

Diverse hypotheses about the climate needed to support the Miocene vegetation in Guajira were explored. The focus was mostly on a key parameter, precipitation, as this is a better predictor than temperature for

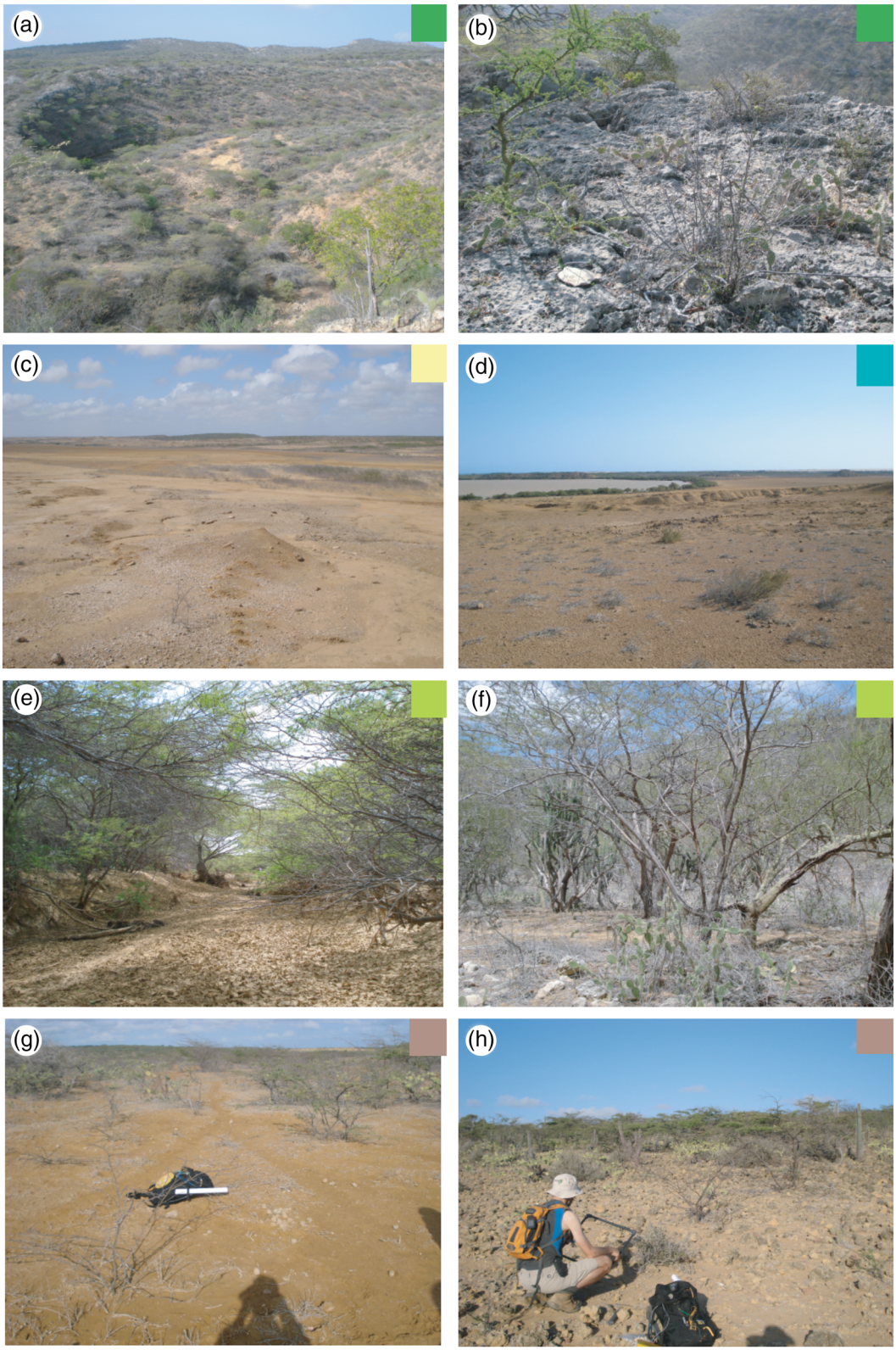

Figure 2. Main modern types of forest in the Cocinetas Basin (Guajira Peninsula). (a) and (b) woodland in the vicinity of Arroyo Ekieps, (c) desert, (d) desert with mangrove bordering the coastline near Tucacas Bay, (e) and (f) thorn forest and woodland along Arroyo Kuluts, and (g) and (h) xerophytic shrublands in Patajau Valley. For location of reference sites and class color codes at the upper right corner of each photo, refer to Figure 1.

the type of forest within tropical latitudes (Jaramillo, 2019; Jaramillo & Cardenas, 2013). We explored published climate sensitivity studies done with global climate models (GCMs) to quantify the effects of several Miocene forcings on precipitation over Guajira during the Neogene.

2. Methods

2.1. Palynology and Micropaleontology

We analyzed the palynological contents of 30 samples including 20 ditch-cutting samples from Well A (labeled as WA from now on; lat 11.9, long −71.3) and 10 surficial samples from the sediment/water interface (Figure 1). We used the surficial samples to establish a palynological baseline for modern/Holocene vegetation that could be compared with the Miocene palynological record. The samples were prepared following standard palynological techniques at IIES-Universidad de Caldas (Traverse, 2007). The procedure included digesting 15 g of rock in hydrochloric acid for 12 hr to remove calcareous material. Hydrofluoric acid was then added to remove silicates. The resulting residue was passed initially through a 250 μm mesh sieve to eliminate the coarse fraction, followed by sieving through a 10 μm mesh. We prepared an extra slide of the fraction that went through the 10 μm mesh as a control to verify that smaller grains were not being discarded. The pollen content of the <10 μm fraction was negligible. The organic residue was cleaned with ultrasonic equipment for some seconds, and then concentrated by centrifugation, followed by mounting of a first cover slide in a solution of polyvinyl alcohol. A second cover slide was mounted following the same protocol described above after oxidation of the residue with nitric acid (HNO_3). Canadian balsam was used to seal both mounted slides. Both biological bright light and differential interference contrast (DIC) microphotographs were obtained at 100× magnification using a Nikon DS-Ri1. The magnification of the camera lens of the Nikon scope was 0.7×, yielding a final magnification of ×700 unless indicated otherwise (supporting information Data Set S2). Each photograph displays its own scale (in microns) because the photographs in each plate are not to the same scale. Photographs were alphabetically sorted into families, genera, and species. Marine palynomorphs were analyzed only in the unoxidized residues to avoid bias due to selective degradation as some peridinoid dinoflagellate cyst taxa are susceptible to degradation during the oxidation stage (Dale, 1976). All marine palynomorphs (dinoflagellate cysts, acritarchs, and microforaminiferal test linings) in the unoxidized residues were counted. Palynological slides are stored at the Smithsonian Tropical Research Institute, Panama.

Pollen and spores were identified to the species level or assigned to an informal species if they had not been formally described. Three hundred palynomorphs were counted per sample when possible. For taxonomic identification of fossil pollen we consulted works on Cenozoic palynology of northern South America (Germeraad et al., 1968; Hoorn, 1994; Jaramillo et al., 2011, 2014, 2017; Lorente, 1986; Muller et al., 1987; Silva-Caminha et al., 2010; Soares et al., 2017) and an electronic database (Jaramillo & Rueda, 2019), which has up-to-date information on pollen and spores from the Cretaceous and Cenozoic for northern South America. Identification of the Holocene pollen types was based on the pollen reference collection of Alan Graham (Moreno et al., 2014) and a small palynological collection from the most abundant plant species in the Cocinetas Basin. We also consulted the works of Lorente (1986), Roubik and Moreno (1991), Colinvaux et al. (1999), and Bush and Weng (2007). Holocene palynomorphs were also named according to the taxonomy used for Miocene palynomorphs in order to enable comparisons between the assemblages. A non-metric multidimensional scaling analysis (NMDS) with Bray-Curtis distance measure was performed to compare the Miocene and Holocene palynological assemblages. The NMDS was performed using the function metaMDS from the package Vegan (R-Development-Core-Team, 2019) in R environment (R-Development-Core-Team, 2019).

The samples analyzed for foraminifera were prepared with water and hydrogen peroxide (Thomas & Murney, 1985) and were washed with neutral soap using a 63 μm sieve. The sediment was dried at approximately 50°C for 24 hr and then sieved in a 125 μm sieve. All planktonic foraminifera were picked from the >125 μm fraction and grouped and sorted onto a micropaleontological slide. Counting was done through a Nikon SMZ1500 stereomicroscope. Taxonomic identification of planktonic foraminifera followed the guides of Kennett and Srinivasan (1983), Young et al. (2017), and Wade et al. (2018) and biozones followed Wade et al. (2011).

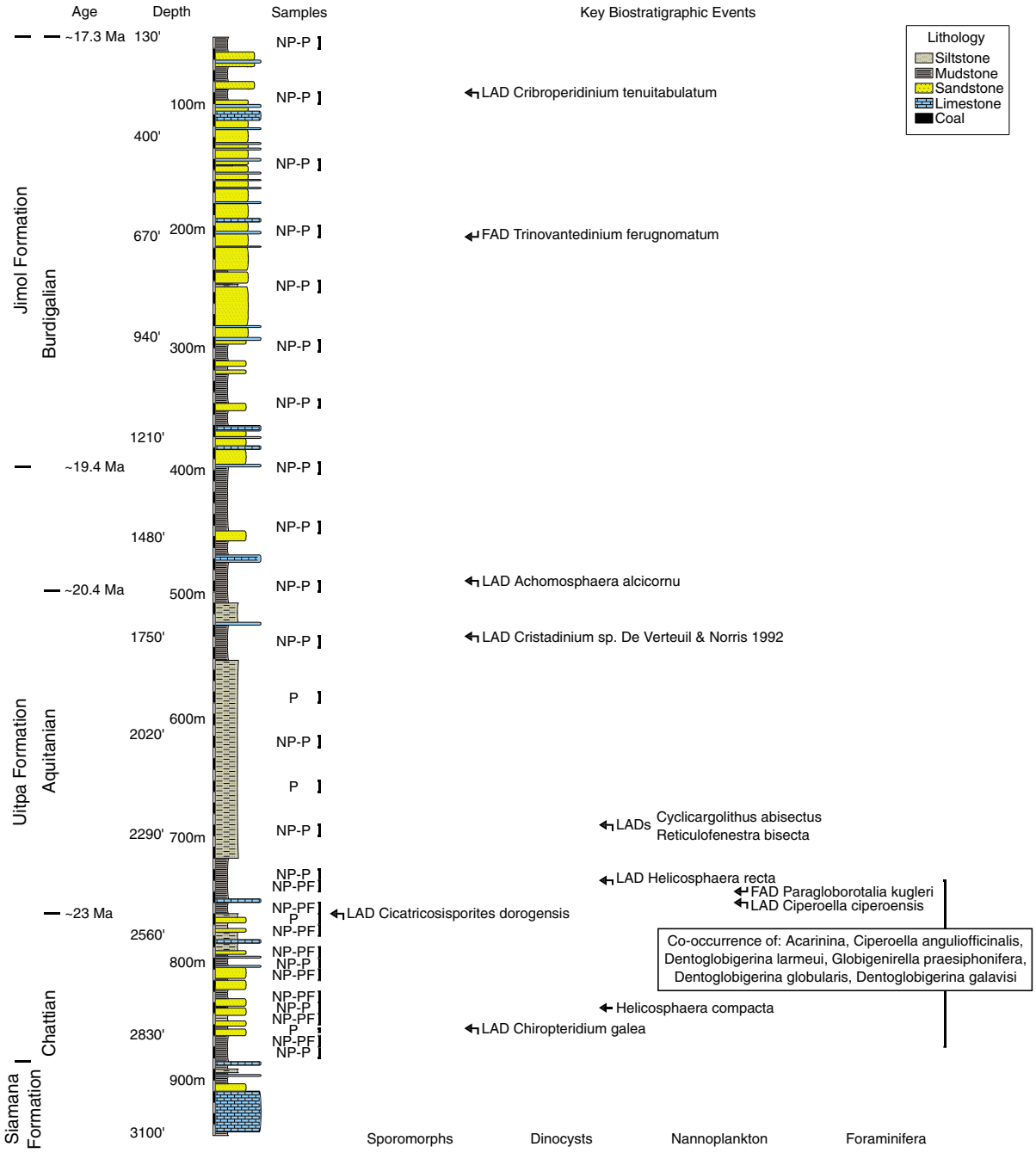

Figure 3. Lithostratigraphy, biostratigraphy, and chronostratigraphy of the late Oligocene-early Miocene WA sequence. Bioevents of calcareous nannoplankton (NP), planktonic foraminifera (PF), and palynomorphs (P). The ages for the top of the WA sequence (~17.3 Ma) and the top of the Uitpa Formation (~19.4 Ma) were extrapolated from $^{87}Sr/^{86}Sr$ isotopic chronostratigraphy from the Cocinetas Basin (Hendy et al., 2015). Oligocene/Miocene boundary based on *Cicatricosisporites dorogensis* LAD (23.03 Ma, Jaramillo et al., 2011).

Calcareous nannofossil slides were prepared using the standard technique of smear slides (Backman & Shackleton, 1983; Young, 1998). The slides were analyzed using a Nikon light microscope at 1000× magnification. Up to 500 coccoliths were counted or a minimum of 200 when scarce. This counting method guarantees at a 99.5% confidence level that specimens representing a minimum of 1% of an assemblage are included (Fatela & Taborda, 2002). We applied the standard biozonation of Martini (Martini, 1971) and the biochronology followed Backman (Backman et al., 2012).

2.2. Lithostratigraphy of Cocinetas Basin

The latitudinal position of the Cocinetas Basin during the Neogene has not changed substantially, 20 million years ago being at 9.5°N while its modern position is at 11.5°N (Montes et al., 2019a, 2019b). Its Cenozoic stratigraphy, which was studied in WA, encompasses an Oligocene-Miocene mixed carbonate-siliciclastic sequence which comprises the Siamana, Uitpa, and Jimol Formations (Figure 3). The Siamana Formation consists of a carbonate reef deposited along the tropical southeastern Circum-Caribbean realm (Silva-Tamayo et al., 2017). The Siamana Formation in WA spans the lowermost 59.4 m of the well and consists of a thick limestone overlain by mixed carbonate-siliciclastics (Figure 3). The boundary between the Siamana and Uitpa Formations is at ~885.4 m (2905′). The Uitpa Formation, which overlies the Siamana, comprises ~492.3 m in WA, and it is composed of a thick sequence of mudstones and siltstones interbedded with thin sandstones and limestones towards the base (Figure 3). The boundary between Uitpa and Jimol is at ~393.2 m (1290′). The Jimol Formation, which overlie Uitpa, comprises a ~353.6 m thick sequence of sandstones interbedded with minor limestones and mudstones (Figure 3). Recent studies in the Cocinetas Basin indicate that the fine-grained siliciclastics of Uitpa were deposited in middle to outer shelf environments (100–200 m water depth) (Carrillo-Briceño et al., 2016; Hendy et al., 2015), whereas the coarse-grained siliciclastics of Jimol were deposited in shoreface to inner shelf environments (<50 m water-depth) (Moreno et al., 2015).

2.3. Vegetation Analysis

The modern vegetation of the Cocinetas Basin is dominated by xerophytic vegetation. In order to better understand the extant distribution of the major types of vegetation in the Cocinetas Basin, we generated a modern ecosystems map following the classification proposed by Mass and Burgos (2011) for seasonally dry tropical forests which is based on the combined effect of soil water availability and potential evaporation/precipitation ratio or *dryness index*. At the local level, the *dryness index* determines the type of flora present at each site. We used field data (i.e., species composition and degree of canopy closure), high-resolution satellite imagery (Geoeye), and Google Earth to generate a set of training points for each of the ecosystem types present in the study area (minimum of 30 points per class) (Figures 2 and S2 and Table 1). We included mangrove as an additional class, owing to its presence along the coast. We used all the training points within a random forest classification (Breiman, 2001) to predict ecosystem class from the following independent variables: elevation, slope, distance to coastline, distance to streams, geologic units, soils, land cover, reflectance from a Spot-5 image bands, and normalized difference vegetation index (NDVI) (Figure S2). All rasters were generated/resampled to match the spatial resolution of the Spot imagery (i.e., 10 m) and were subset to our area of interest. For each training point, values of all independent variables were extracted and used as input for the random forest R package (Liaw & Wiener, 2002). This tool generates a large number of decision trees (i.e., forest) based on a bootstrap subset of the training samples. Subsequently, each pixel in need of classification is put down in each tree and assigned to a class. The final class is selected as the one having the majority vote. Classification error is performed internally using the training samples left out of the bootstrap subset (Breiman, 2001). During the classification process, we excluded soils, near-infrared reflectance and green band reflectance, since these variables were either highly correlated with others or did not significantly improve the classification accuracy. Spatial data processing was performed in IDRISI (Clark Labs) and ArcGIS (ESRI), and statistical analyses were performed in R (R-Development-Core-Team, 2019).

Some ecologists have suggested that the modern vegetation of Guajira could be an anthropic effect of European colonization from the sixteenth to ninteenth centuries. In order to evaluate for this possibility, we analyzed written accounts of vegetation described by priests and sailors during the first wave of Spanish colonization. We compiled and reviewed sixteenth and seventeenth historical sources (Table S1) that described the principal inland exploration routes between the settlements currently known as *Coro* (founded in 1527), *Cabo de la Vela* (founded in 1536), *Riohacha* (founded in 1538), and *Maracaibo* (founded in 1547) (Figure S1). Using these writings, we searched for specific terms and expressions that described the local vegetation or relevant references to animal and human occupations around the region. Each term or expression was then categorized into “xerophytic,” “savannah,” or “woodland,” based on comparisons to modern ecosystems in the region (Instituto de Hidrología et al., 2017).

Table 1
Modern Ecosystem Map Classes

Ecosystem name[a]	Description at the local level	Dominant species
Woodland	Thicket, dense shrubland growing in rocky areas (e.g., limestone, gneiss)	*Subpilocereus repandus, Castela erecta, Parkinsonia praecox, Bursera simaruba, Rhamnus* sp., *Senna atomaria*
Desert	Open areas without vegetation, with some patches covered by shell beds, or saline soils with sparse small shrubs	Bare, or with *Jatropha gossypiifolia* growing in small patches
Mangrove	Mangrove	*Avicennia* sp.
Thorn forest and woodland	Bushland margins growing along streams	*Pereskia guamacho, Haematoxylum brasiletto, Guaiacum officinale, Cissus* sp., *Prosopis juliflora*
Xerophytic shrubs and scrubs	Open thorn scrub forest	*Opuntia caracassana, Prosopis juliflora, Castela erecta, Subpilocereus repandus*

[a]*Sensu* (Mass & Burgos, 2011).

2.4. Climatic Analysis

To assess the modern climate of the basin, we analyzed monthly precipitation data from 23 IDEAM stations (Colombian Institute for Hydrology, Meteorology and Environmental Studies) over a period of ~40 years (Figure S3). The modern environmental distribution of the taxa represented in the fossil pollen and spore record from WA was described by using the genus-level, georeferenced occurrences reported in BIEN (Maitner et al., 2018) for the respective plant genera. Our training dataset has fewer datapoint in the dry end of the precipitation spectrum (Figure S4) that could produce an overestimation in the precipitation towards the dry end of the moisture gradient. All pollen identifications were taken to generic level to avoid the potential noise from lower taxonomic resolution. Geodetic coordinates of occurrence of each taxon were used to extract both mean annual temperature and precipitation, and daily temperature and annual temperature ranges from the WorldClim dataset (Hijmans et al., 2005). We used the mean annual temperature and precipitation of the occurrence points of each taxon to estimate a bivariate probability density function (*pdf*) (Wand & Jones, 1994) describing the taxon's distribution across the environmental space defined by temperature and precipitation. A second *pdf* was estimated for each taxon using daily and annual temperature ranges. For each fossil sample, the *pdf*s of the taxa present in the sample were submitted to an unweighted mixture, producing an overview of the probable conditions at the time the pollen assemblage was deposited. Summarizing, taxon level bivariate *pdf*s were used to derive sample *pdf*s. The environmental space associated with the upper 0.05 of probability for either taxa or samples was considered representative of the climate where the taxa are most likely to occur, and therefore, in the case of samples, the most likely climate at the moment of sample deposition. Thus, it was possible to illustrate taxa and sample distributions in a single environmental space. Miocene and Holocene climate estimates were summarized by adding the *pdf*s associated with samples from each epoch.

We then explored diverse hypotheses about the type of climate needed to support the vegetation in Guajira during the Miocene, in the light of recent knowledge regarding present-day climate dynamics of the region and numerical climate simulations for the Miocene. We also explored published climate sensitivity studies (all variables stay the same and only the variable of interest changes) to assess the effect of two key events in Earth history (the rise of the Andes and closure of the Central Panama Seaway) on Guajira's climate.

3. Results

3.1. Biostratigraphy

The closest outcrop section to WA is La Tienda, Locality ID 290432 (Moreno et al., 2015). The base of La Tienda is ~400 m northwest of WA where the dip of strata is very shallow (~3.5°SE), and consequently, the top of WA is correlated with the lowermost limestone of the Jimol Formation in La Tienda, ~60 m depth in the composite section for the basin (Moreno et al., 2015). The lower boundary of the Jimol Formation at WA is at 393.2 m (1290′) based on the thick coarse-grained mixed carbonate-siliciclastic package (~30.4 m thick) capping the fine-grained siliciclastics of the upper Uitpa Formation (Figure 2). The Jimol Formation, consequently, would be ~393.2 m thick at WA whereas Utipa would be ~368.8 m thick

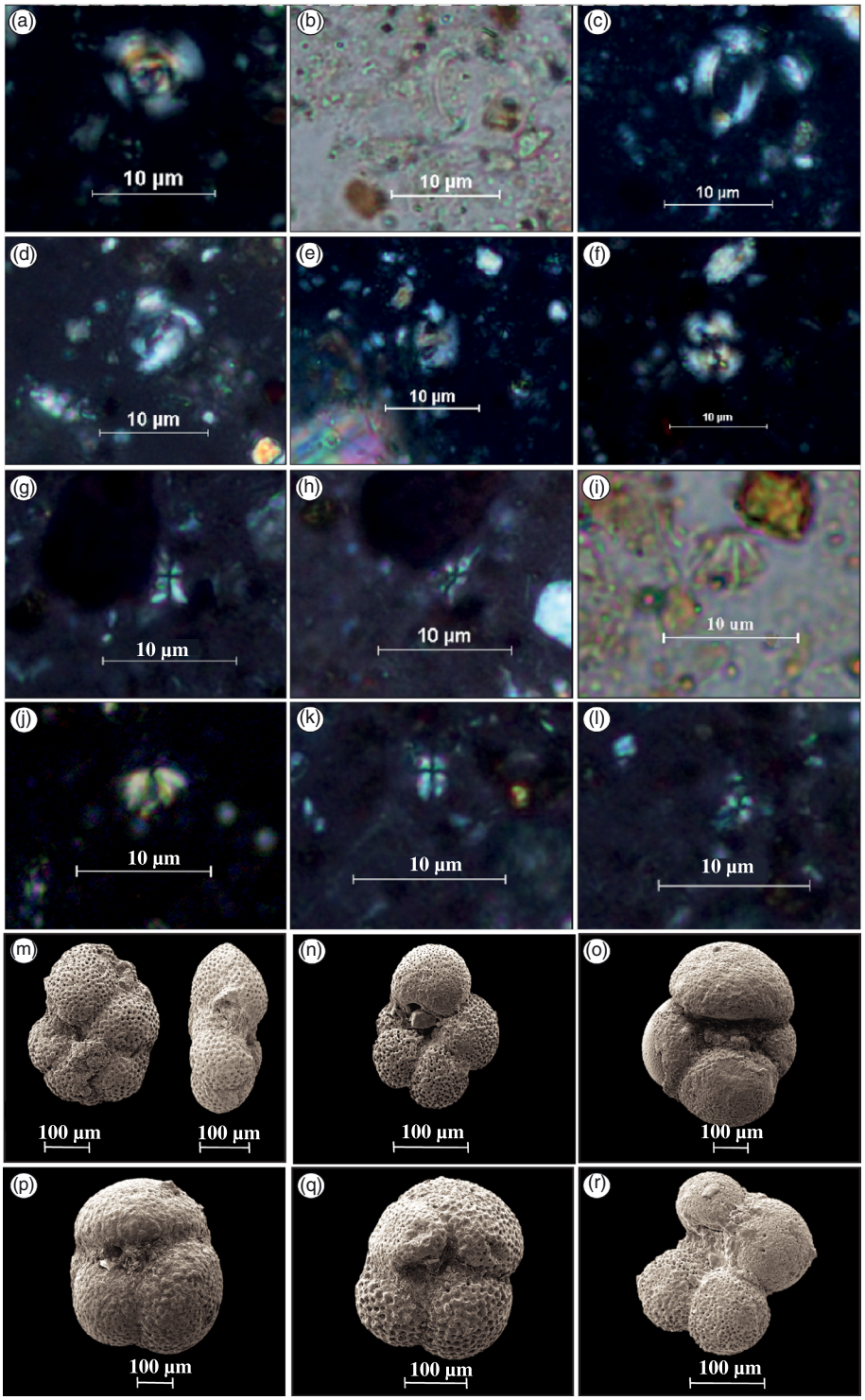

Figure 4. Selected calcareous nannofossils and planktonic foraminifera. (a) *Cyclicargolithus abisectu* (2740–2770′). (b) and (c) *Helicosphaera ampliaperta* (130–160′). (d) *Helicosphaera compacta* (2740–2770′). (e) *Helicosphaera recta* (2860–2890′). (f) *Reticulofenestra bisecta* (2260–2290′). (g) and (h) *Sphenolithus belemnos* (1440–1470′). (i) and (j) *Sphenolithus umbrellus* (2830–2860′). (k) and (l) *Sphenolithus disbelemnos* (1440–1470′). (m) *Paragloborotalia* cf. *kugleri* (2410–2440′). (n) *Ciperoella ciperoensis* (2710–2740′). (o) *Dentoglobigerina globularis* (2470–2500′). (p) *Dentoglobigerina galavisi* (2650–2680′). (q) *Dentoglobigerina larmeui* (2710–2740′). (r) *Globigerinella* cf. *praesiphonifera* (2710–2740′).

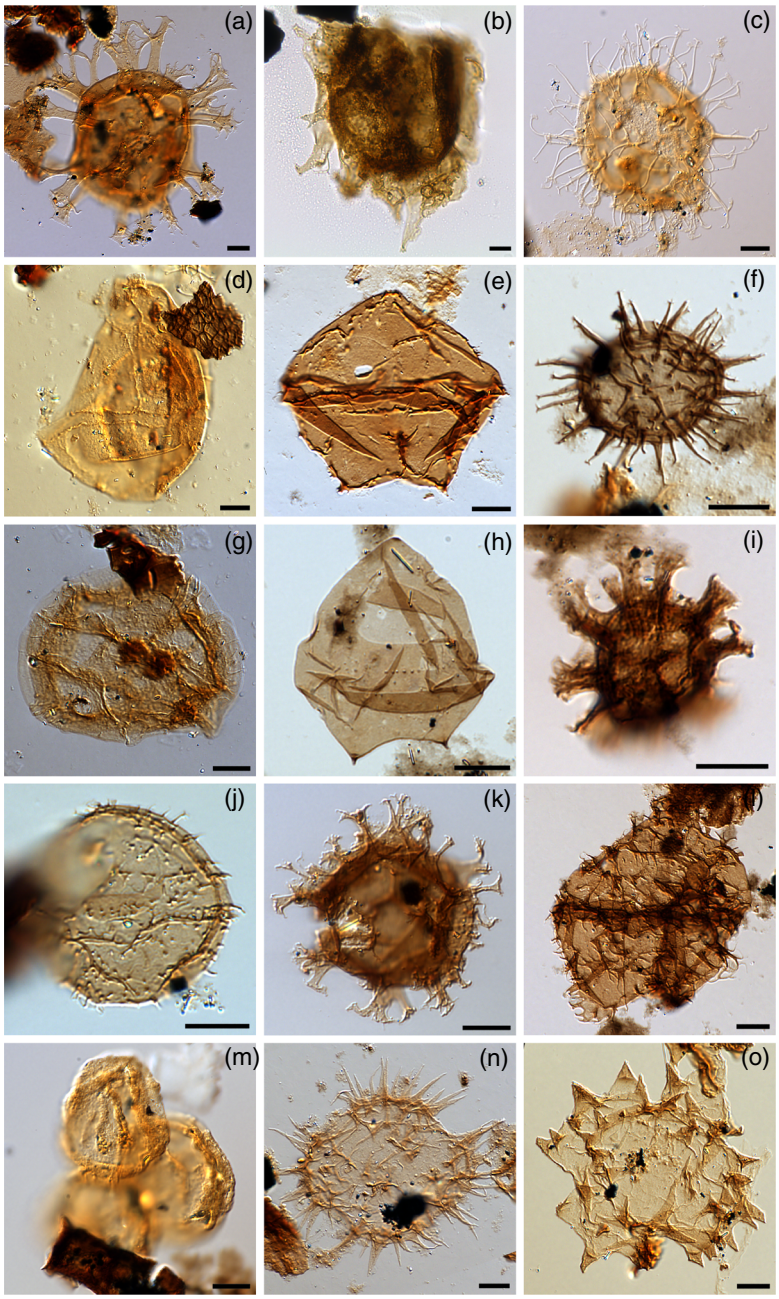

Figure 5. Photographs of selected dinocysts (a–l) and acritarchs (m–o) in WA. Scale bar is 10 μm. E.F.: England Finder coordinates. (a) *Achomosphaera alcicornu*, uncertain view, high focus on processes. 1600′–1630′, EF: F40/3. (b) *Chiropteridium galea*, ventral view, high focus on processes. 2810′–2820′, EF: M67/2 (c) *Cleistosphaeridinium diversispinosum*, uncertain view, mid-focus on processes. 130′–160′, EF: H42/2. (d) *Cribroperidinium tenuitabulatum*, right lateral view, high focus on wall and archeopyle margin. 640′–670′, EF: L48. (e) *Cristadinium* sp. of De Verteuil and Norris (1992), dorsal view, mid-focus on wall and archeopyle suture. 2020′–2050′, EF: K48/4. (f) *Echinidinium euaxum*, uncertain view, low focus on processes. 1750′–1780′, EF: J34/2. (g) *Heteraulacacysta campanula*, apical view, high focus on wall and archeopyle. 460′–490′, EF: D25. (h) *Lejeunecysta marieae*, dorsal view, mid-focus on archeopyle. 1750′–1780′, EF: N36. (i) *Minisphaeridium latirictum*, apical view, high focus on archeopyle. 2140′–2170′, EF: E43/2. (j) *Trinovantedinium ferugnomatum*, dorsal view, low focus on processes and archeopyle suture. 130′–160′, EF: K32/2. (k) *Trinovantedinium variabile*, uncertain view, high focus on processes. 1600′–1630′, EF: L32/2. (l) *Trinovantedinium*? *xylochoporum*, ventral view, mid-focus on wall and processes. 2140′–2170′, EF: V38/3. (m) *Cyclopsiella elliptica/granosa* complex, uncertain view, high focus on wall. 1900′–1930′, EF: H37/3. (n) *Quadrina*? *condita*, uncertain view, mid-focus on wall and processes. 2020′–2050′, EF: X28/1. (o) *Quadrina* "incerta" of Jaramillo et al. (2017), uncertain view, mid-focus on wall and processes. 280′–310′, EF: S37/1.

Table 2
Most Abundant Taxa in Palynological Samples

Miocene		Holocene	
Family	Genus	Family	Genus
Arecaceae	Arecaceae	Cyperaceae	aff. *Eleocharis*
Bignoniaceae	*Arrabidaea*	Amaranthaceae	Amaranthaceae
Bataceae	*Batis*	Simaroubaceae	*Castela*
Betulaceae	Betulaceae	Fabaceae-Pap.	cf. *Myrocarpus*
Malvaceae-Bom	Bombacoideae sp2	Fabaceae	Fabaceae sp2
Fabaceae-Caes.	Caesalpinioideae sp2	Cactaceae	*Opuntia*
Meliaceae	*Cedrela*	Amaranthaceae	*Philoxerus*
Cyatheaceae	*Cyathea* 1	Poaceae	Poaceae
Cyatheaceae	Cyatheaceae sp1	Rhizophoraceae	*Rhizophora*
Alismataceae	*Echinodorus*	Cyperaceae	Unknown
Malpighiaceae	*Hiraea*	Urticaceae	Urticaceae
Euphorbiaceae	*Hura*		
Arecaceae	*Lepidocaryum*		
Polypodiaceae	*Polypodium*		
Sapotaceae	*Pouteria*		

(Figure 2). The boundary between Siamana and Uitpa in WA corresponds to a sharp lithological limestone/shale contrast at 885.4 m (2905′) (Figure 3).

Important biostratigraphic taxa includes the calcareous nannofossil *Helicosphaera ampliaperta* at the top of WA (Figure 4 and supporting information Data Set S1), the last appearance datum (LAD) of planktonic foraminifera *Ciperoella ciperoensis* at 752.9 m (2470′), the LAD of spore *Cicatricosisporites dorogensis* at 762 m (2500′), a single occurrence of *Paragloborotalia* cf. *P. kugleri* at 734.6 m (2410′), the co-occurrence in the interval 734.6–871.7 m (2410′–2860′) of planktonic foraminifera *Dentoglobigerina galavisi*, *Dentoglobigerina globularis*, *Dentoglobigerina larmeui*, and *Globigerinella praesiphonifera*, the occurrence of *Helicosphaera compacta* at 835.2–844.3 m (2740′-2770′), the occurrences of *Cyclicargoliyhus abisectus* at 688.9–871.7 m (2260′–2860′) and *Sphenolithus umbrellus* at 752.9–798.6 m (2470′–2620′), the LAD of both *Cyclicargoliyhus abisectus* and *Reticulofenestra bisecta* at 688.9 m (2260′), and the sporadic occurrence of *Helicosphaera recta* at 734.6–880.9 m (2410′–2890′). There are occurrences of *Sphenolitus belemnos* from 438.9 m (1440′) to 734.6 m (2410′); the LADs of the dinocysts *Chiropteridium galea* is at 856.5 m (2810′) and *Achomosphaera alcicornu* is at 487.7 m (1600′) (Figure 5 and supporting information Data Set S1). *Cleistosphaeridium diversispinosum* was recorded throughout the entire WA sequence. The LAD of *Cribroperidinium tenuitabulatum* occurs at 85.3 m (280′) and the FAD of *Trinovantedinium ferugnomatum* at 204.2 m (670′). The LAD of *Cristadinium* sp. of De Verteuil and Norris (1992) occurs at 533.4 m (1750′), and there is a single occurrence at 85.3 m (280′) of *Quadrina* "incerta" of Jaramillo et al. (2017). The LAD of *Quadrina*? *condita* is at 615.7 m (2020′).

3.2. Contrasts in Vegetation From Miocene to Present in La Guajira

There are two main dry-forest types in the Cocinetas Basin, the desert and xerophytic shrubs and scrubs (Figure 2 and Table 1), and these occupy more than 90% of the basin's area (Figure 1). Additional types of dry forest include the thorn forest and woodland occurring along the water courses and the woodlands that occur in the mountains surrounding the basin (Figure 1). There is a fifth type of vegetation, mangrove, which occurs in the intertidal zones. The accuracy of land cover classification was 96%, and ranged from 93% (thorn forest and woodland, xerophytic shrubs, and scrubs) to 100% (mountain woodland and mangrove). Overall, the most important variables in explaining ecosystem distribution were red-band reflectance, normalized difference vegetation index (NDVI), and elevation, although there were other variables important at the individual class level. For instance, geology was among the three most important variables for mountain woodland distribution, whereas distance to the coastline was important for mangroves (Figure 1).

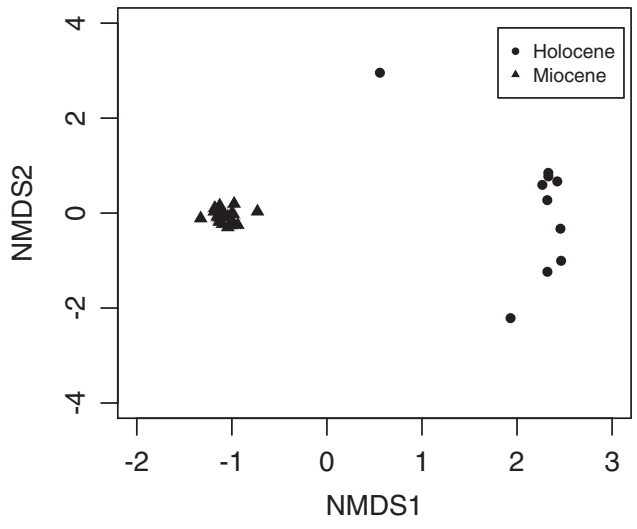

Figure 6. Non-metric multidimensional scaling (NMDS) of the Miocene and Holocene pollen samples.

Historical accounts consistently described the areas surrounding northern Guajira (*Cabo de la Vela*) as extensive landscapes of arid soils and poor vegetation of thistles and thorns; 64.8% of all the terms that describe the environment are related to xerophytic assemblages and 19.4% to savanna (Table S1). The remaining 15.8% of environmental terms indicate woodland ecosystems that resemble the vegetation found in the sierras located in the northeastern and southeastern parts of the peninsula today.

Out of a total of 8,272 palynomorphs counted, we identified 206 taxa, including 120 angiosperms, 1 gymnosperm, 20 ferns, 51 dinoflagellate cysts, and 14 reworked taxa (for a complete list of the fossil taxa, full counts and illustration of 103 taxa in three plates, see supporting information Data Sets S1 and S2). The early Miocene pollen record is dominated by ferns (e.g., *Polypodium* and *Cyatheacaee*), large tropical trees (*Arrabidea, Hura, Hiraea, Bombacoideae, Caesalpiniodeae, Pouteria*,

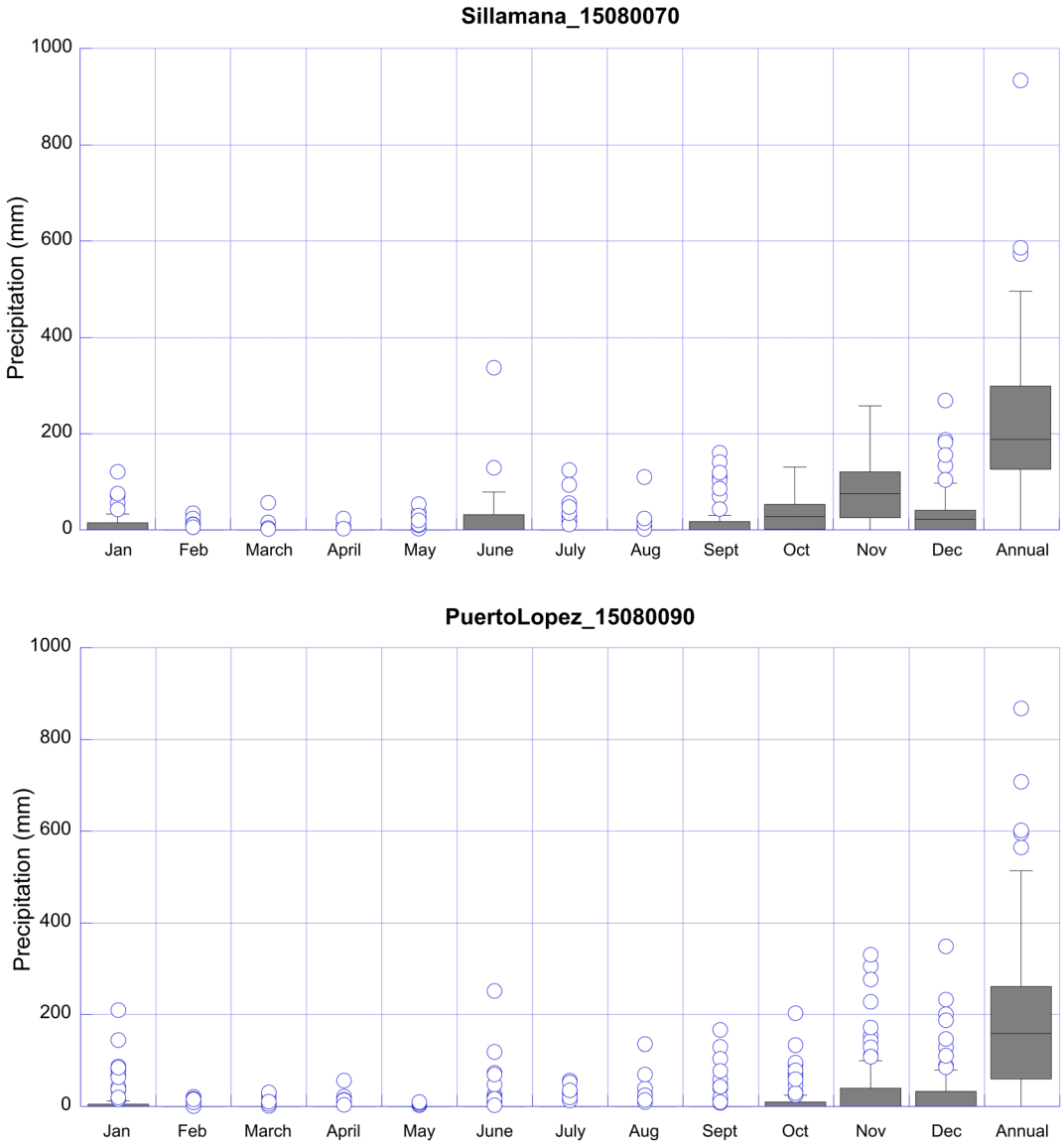

Figure 7. Boxplot of mean monthly and annual precipitation (1972–2018) for the Sillamana and Puerto Lopez stations in northeast Guajira Peninsula. Data from the Colombian Institute of Hydrology, Meteorology and Environmental Studies (IDEAM) were downloaded online (http://dhime.ideam.gov.co/atencionciudadano/).

and *Cedrela*), and palms (*Lepidocaryum/Mauritia*) (Table 2 and Data Set S1). The Holocene pollen record is dominated by shrubs and herbs including *Castela*, Urticaceae, *Myrocarpus*, *Eleocharis*, *Philoxerus, Cyperaceae*, Amaranthaceae, *Poaceae*, and *Opuntia* (Table 2 and Data Sets S1 and S2). The NMDS (Figure 6) had a low stress value (0.07), and Miocene samples are significantly separated from Holocene samples along axis 1 (*t* test, mean NMDS axis 1 score for Miocene −1.09, mean NMDS axis 1 score for Holocene 2.13, $p < 0.001$, df = 9.4).

3.3. Climate

Modern climate in the northern Guajira Peninsula is characterized by year-round high temperatures with little monthly variability. The mean annual temperature (MAT) is 26.0°C, with a range of monthly mean values of only ~3.0°C. The mean annual precipitation (MAP) ranges from 218 to 532 mm. There is a slight latitudinal gradient in MAP, with higher values on the southern part of the Peninsula and around the Macuira mountain range. Intra-annual (seasonal) rainfall variability is pronounced, regardless of the

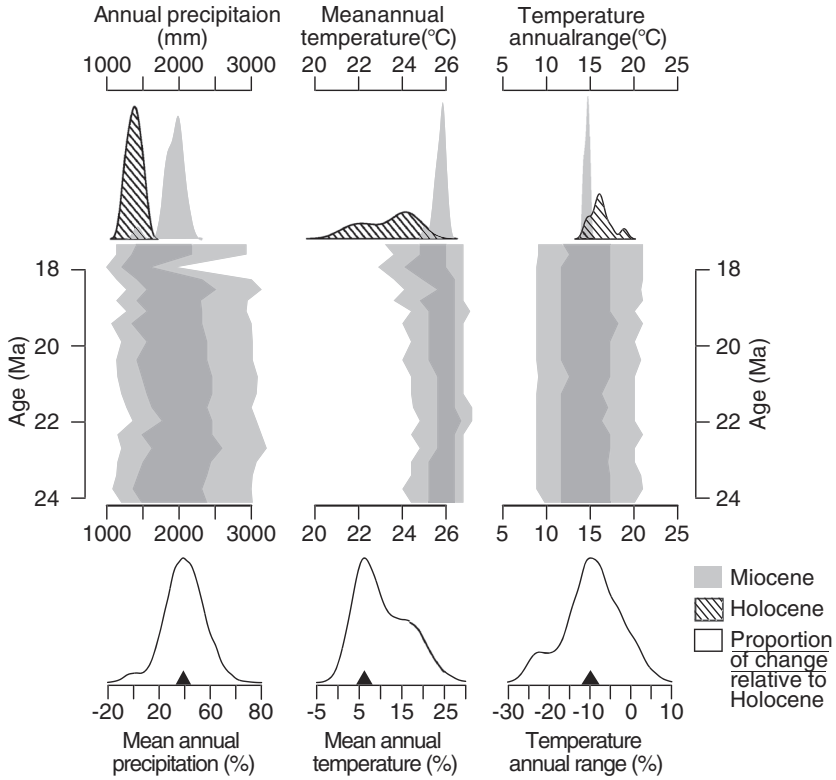

Figure 8. Estimations of mean annual temperature and mean annual precipitation for the Guajira Peninsula during the Miocene and Holocene. Dark and light gray bands show interquartile range (50% of central probability) and 95% confidence interval of the reconstructed environmental attributes, respectively. The upper probability density functions (pdf) show the comparison of average conditions during the Holocene (dashed polygons) and the Miocene (gray polygons) whereas the lower pdfs show the percentual difference of change of the Miocene relative to the Holocene (gray triangles show the difference associated with the highest probability density).

geographic location on the Peninsula. There is a short wet season between September and December. Highest rainfall values are recorded in November, with median montly values always <150 mm at all locations. The short humid season is followed by an 8- to 9-month dry period, interrupted only by a brief increase in precipitation during June. The only two meteorological stations in the Cocinetas Basin record a very low MAP, 236 mm for Sillamana and 218 mm for Puerto Lopez (Figures 7 and S3). Most rivers are small and seasonal, being dry most of the year. There are very few lakes and those that persist year-long are highly saline.

The climatic estimations derived from the palynological content of the samples indicate a MAP of 1,300 mm for the Holocene and 2,000 mm for the Miocene, a significant increase of 40% (Figure 8). The MAT for the Holocene is ~24°C, whereas it is ~26°C for the Miocene (Figure 8).

4. Discussion

4.1. Biostratigraphy

The early Neogene of the Cocinetas Basin is poorly studied and consequently information on its geochronology is imprecise. Therefore, a large focus of our study was on dating the stratigraphic section, because age is a critical component of any paleoclimatic analysis. Well WA encompasses the upper Siamana, Uitpa and lower Jimol formations, and of these, only the Jimol has previous studies with a solid time control. Using molluscan Sr stratigraphy, Hendy et al. (2015) determined the age of the uppermost part of WA (39.6 m) to be ~17.3 Ma (Figure 3) and that of the Uitpa-Jimol contact, which is at 393.2 m (1290′) to be 19.4 Ma (Figure 3, supporting information Section S1). The presence of the calcareous nannofossil *Helicosphaera*

ampliaperta (20.43–14.86 Ma) (Backman et al., 2012) at the top of WA also supports a Burdigalian age for the upper segment.

An important datum is the stratigraphic position of the Oligocene/Miocene boundary in the basin, which has been a matter of dispute for more than 70 years (see detailed discussion in Section S1 and Data Set S1). Several biostratigraphic datums establish the position of the boundary in WA at 762 m (2500′); these include the LAD of *Ciperoella ciperoensis*, *Cicatricosisporites dorogensis*, the co-occurrence of *Dentoglobigerina galavisi*, *D. globularis*, *D. larmeui*, and *Globigerinella praesiphonifera*, the occurrence of *Helicosphaera compacta* and the LAD of both *Cyclicargoliyhus abisectus* and *Reticulofenestra bisecta* (Data Set S1 and see supporting information for a more extensive explanation). Assuming a constant sedimentation rate within the middle/upper Uitpa and using the top of the Oligocene at 762 m (2500′) and 19.4 Ma at 393.2 m (1290′), the Aquitanian/Burdigalian boundary would be at ~495.6 m (1626′).

Overall, the biostratigraphic analysis indicates that the WA section extends from the latest Oligocene to early Miocene (late Chattian to Burdigalian) (Figure 3). The top of the Siamana Formation is late Chattian (late Oligocene), and the Uitpa Formation extends from the latest Oligocene to the early Burdigalian (~19.4 Ma). Well A started drilling in the lower part of the Jimol Formation at a stratigraphic level dated as Burdigalian (~17.3 Ma).

4.2. Vegetation and Climate

Since 1499 and during the first two centuries of European colonization of the Americas, the *Cabo de la Vela* in the Guajira Peninsula, about 60 km northeast of the Cocinetas Basin, was one of the main strategic points for commercial routes and exploration (Polo Acuña, 1998). Detailed accounts from the captains, friars and officials found in *Relaciones Geográficas*, *visitas de encomiendas* and *elegías* during the sixteenth and seventeenth centuries provide descriptions of the human and ecological environments during the initial stages of Spanish colonization (Bürgi et al., 2004; Butzer & Butzert, 1997; Endfield & O'Hara, 1999; Etter et al., 2006; Tovar, 1992; Turner & Butzer, 1992). During this time, extensive exploration for and exploitation of pearls and gold became the main drivers of commerce and communication routes (Barrera, 2000; Navarrete Peláez, 2003; Vásquez & Correa, 1993). The xerophytic and woodland vegetation types described near *Cabo de la Vela* (Table S1) are consistent with the vegetation that exists in Guajira today (Figures 1 and 2). The historical accounts indicate that modern vegetation is indeed natural and not a byproduct of drastic human modification.

The modern vegetation of the Cocinetas Basin is dominated by desert and xerophytic shrubs and scrubs (Figure 2 and Table 1), which account for more than 90% of basin's area (Figure 1). The desert type is mostly bare land with occasional monotypic patches of the shrub species *Jatropha gossypiifolia* (Euphorbiacea) and the xerophytic shrubs/scrubs type is dominated by the cactus *Opuntia* and the thorny legume *Prosopis* (Table 1). The Holocene palynological record largely reflects the modern vegetation (Table 2 and Data Set S1). In contrast, the early Miocene palynological record is significantly different from Holocene palynofloras (Figure 6). Early Miocene palynofloras have many floristic elements from tropical rainforests (Table 2) including *Cedrela, Hura*, Bumbacoideae, *Pouteria*, and many palms including *Lepydocarium* and *Mauritiella*. Sediments from the Uitpa Formation are shallow marine, and consequently, most of the pollen and spores recorded in this study were transported from the land by currents and perhaps also by wind, although in lower proportion, as occurs in the modern Orinoco Delta (Hofmann, 2002; Muller, 1959). It could be argued that a long river with a large catchment basin that included tropical rainforest hundreds of kilometers to the south was delivering sediments and pollen along with it to the Cocinetas Basin. However, provenance analysis in the basin indicates that most sediments were delivered from nearby sources (Perez-Consuegra et al., 2018), thus excluding the possibility of long-distance pollen transport. MAP estimations indicate that during the early Miocene (Figure 8), the region was significantly wetter than during the Holocene, reaching almost 2,000 mm and that it lay within the climatic envelope of modern tropical rainforests (Jaramillo & Cardenas, 2013). The substantial increase in precipitation is also seen in the Middle Miocene record of the same basin (Scholz et al., 2020). Miocene MAT was also warmer, an almost two-degree increase compared to Holocene predicted values (Figure 8). Overall, precipitation, temperature, and floristic composition indicate that the forest surrounding the Cocinetas Basin underwent a profound transformation, from a tropical rainforest in the early Miocene to the modern xeropythic vegetation. The extensive vertebrate record from the middle Miocene Jimol Formation and middle Pliocene Ware

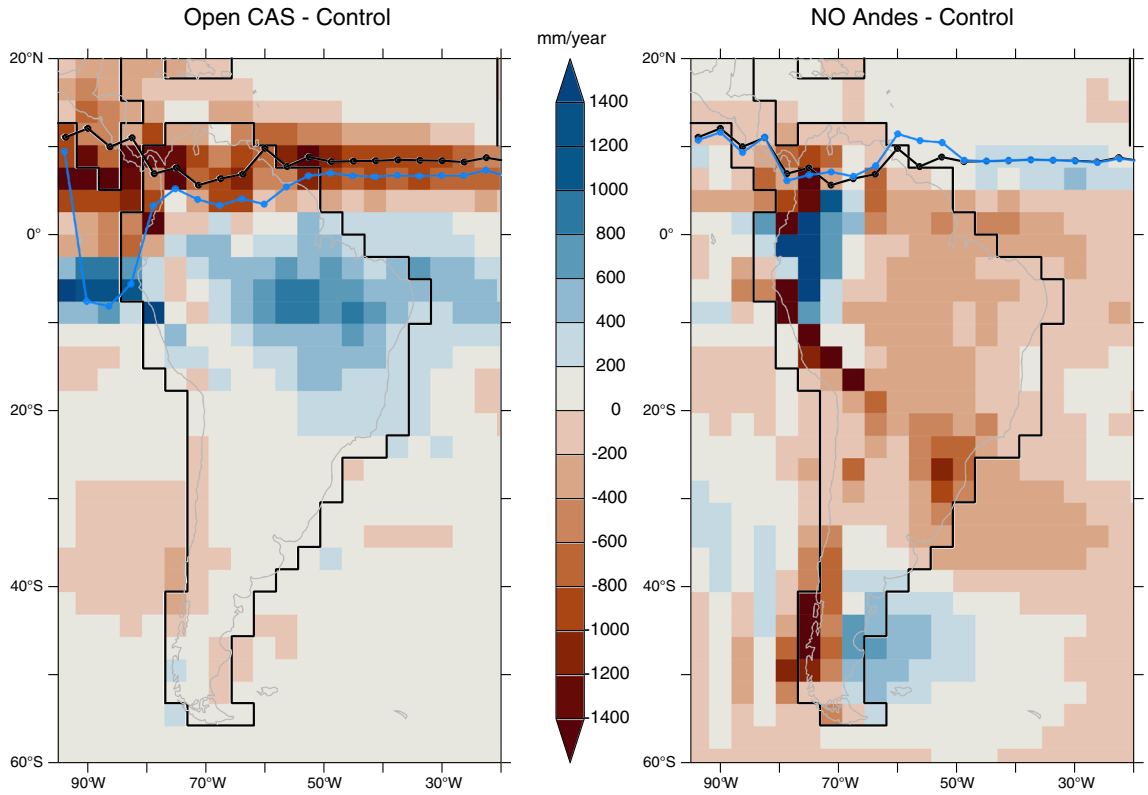

Figure 9. Results from sensitivity experiments carried out with the IPSL-CM4 model. Annual rainfall anomalies between an open Central American Seaway (CAS) experiment and pre-industrial "control" experiment (left) and between an experiment with no Andes and a pre-industrial "control" experiment (right). CAS experiment is described in Sepulchre et al. (2014). The atmospheric-only equivalent to Andes experiment is described in Sepulchre et al. (2010). Black and blue lines indicate the ITCZ northern limit for the control and sensitivity experiments, computed following Braconnot et al. (2007).

formation in the same basin (Aguilera, Lundberg, et al., 2013; Aguilera, Moraes-Santos, et al., 2013; Amson et al., 2016; Cadena & Jaramillo, 2015a, 2015b; Carrillo et al., 2018; Florez et al., 2018a, 2018b; Forasiepi et al., 2014; Jaramillo et al., 2015; Moreno et al., 2015; Moreno-Bernal et al., 2016; Perez et al., 2017; Suarez et al., 2016) suggests that the rainforest and high precipitation persisted to the middle Pliocene. Provenance analysis also indicates that most rivers had local watersheds and that most of the water was derived from precipitation within the Cocinetas Basin (Perez-Consuegra, Parra, et al., 2018).

There is a sedimentary hiatus in Cocinetas during the late Miocene to early Pliocene; however, knowledge about this gap can be informed by the adjacent Falcon province in northwestern Venezuela, which has an extensive sedimentary record of the Late Neogene. The climate and vegetation of Falcon are similar to those of Cocinetas; both belong to the *Caribbean dry plant formation* biogeographic province (Sarmiento, 1975), and the vegetation types of Falcon are similar to those described here (Matteucci, 1987; Matteucci et al., 1982; Medina et al., 1989), as are the temperature and precipitation regimen, both being in the South Caribbean Dry Zone (Martelo, 2003). The extensive vertebrate and sedimentological record of the late Miocene Urumaco Formation in Falcon indicates the existence of a tropical fluvial plain environment with freshwater bodies that range from shallow lakes and ponds to small and large rivers (Lorente, 1986; Quiroz & Jaramillo, 2010; Sánchez-Villagra et al., 2010). The fish fossil record also indicates that permanent freshwater bodies (rivers and lakes) continued at least until the middle Pliocene in both the Falcon province and Cocinetas Basin (Aguilera, Moraes-Santos, et al., 2013). Therefore, the shift to the modern xerophytic condition must have occurred over the past ~3 million years.

Today, moisture transport and rainfall patterns of northern South America are driven "by the confluence of global and local factors" (Hoyos et al., 2018), including large-scale atmospheric dynamics, topography, and continental water recycling. The Guajira Peninsula is located north of the boreal summer limit of the Inter Tropical Convergence Zone (ITCZ), and its climate is instead strongly influenced by the Caribbean

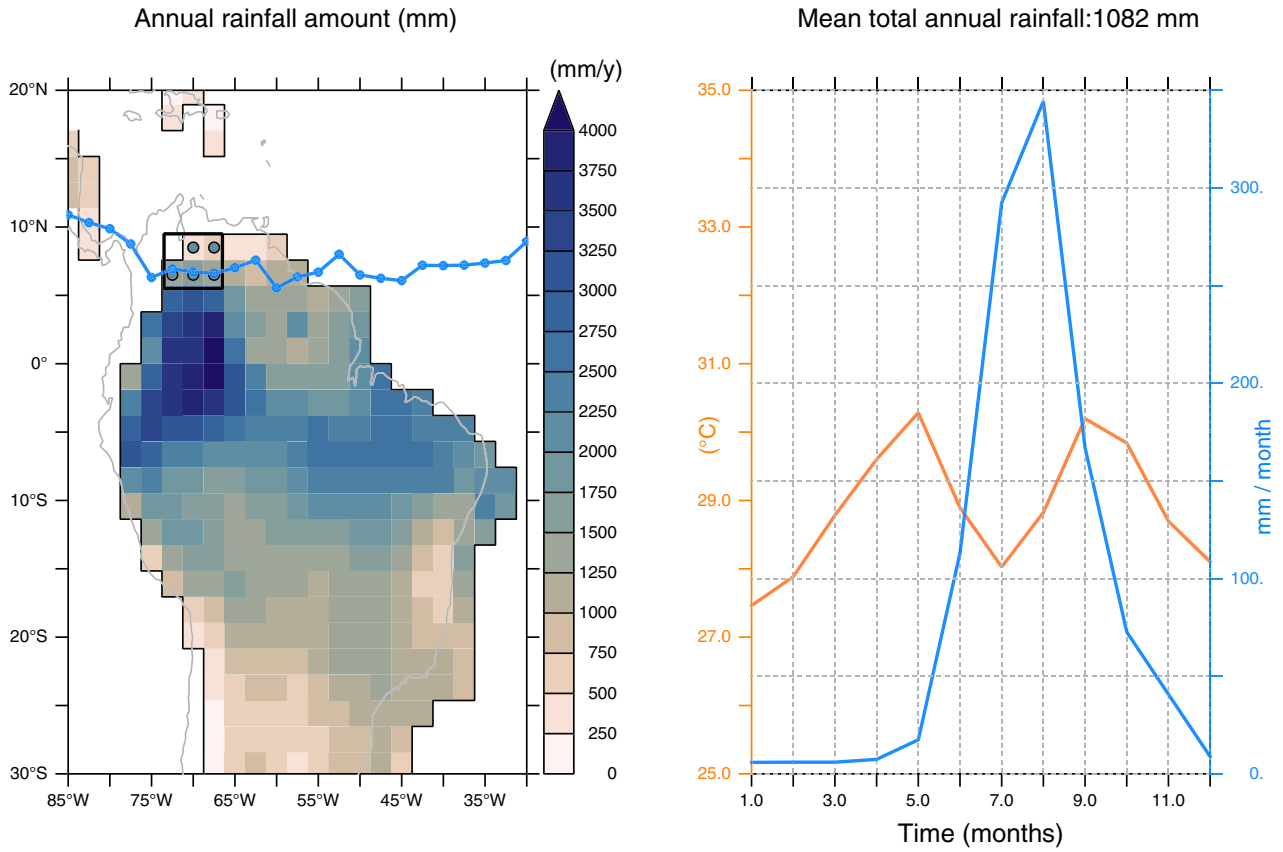

Figure 10. Left. Annual rainfall amount simulated with NCAR CESM model forced with Miocene boundary conditions, described in Zhou et al. (2018). The blue line depict the June-July-August ITCZ northern limit, computed following Braconnot et al. (2007). Right. Seasonal cycle of surface temperature and precipitation, averaged over the northeastern box of South America (black rectangle on left panel).

Low-Level Jet (CLLJ), which corresponds to a maximum of easterly zonal wind in the lower troposphere (Wang, 2007). The CLLJ corresponds to the lower lateral branch of a Walker cell that advects moisture from the eastern Caribbean to central America where convection and rainfall occur. In turn, subsidence and seasonal aridity are set over the eastern part of this cell, including the Guajira Peninsula (Gamble & Curtis, 2008; García-Martínez & Bollasina, 2020). Analyses of moisture divergence from ERA-interim reanalysis (Dee et al., 2011) show that moisture convergence over the Guajira Peninsula occur only from September to December, explaining the rainy season depicted earlier (Hoyos et al., 2018). In line with the strong easterlies associated with the CLLJ, the Guajira Peninsula is adjacent to a strong upwelling system that leads to rather cold sea surface tempatures, thereby reducing evaporation and moisture advection to the continent. Today, apart from moisture advection from the oceans, an important part of the continental rainfall over northern South America comes from the continental recycling. In the case of the Guajira Peninsula, the xerophytic nature of the vegetation impedes strong evapotranspiration fluxes, thereby acting as a positive feedback to aridity. Nonetheless, the Guajira Peninsula is very sensitive to interannual variability in precipitation typically at the time scale of El Niño events (2–4 years); such precipitation changes can result in major changes in vegetation (Figure S5). Therefore, the drastic changes from the Miocene to the Holocene and modern conditions call for identifying drivers of a long-term climate change.

A shifted ITCZ during the Miocene? A first working hypothesis to explain aridification of La Guajira Peninsula between the Miocene and today is a southward shift of the ITCZ. Changes in orbital parameters could be invoked, as summer insolation determines the ITCZ latitudinal position. However the orbital forcing cannot explain the long-term aridification by itself, since numerical experiments with favorable insolation parameters for a northward ITCZ show no change in rainfall patterns over northern South America (Liu et al., 2017). The Miocene earth system is characterized by conditions very different from

today's, including atmospheric pCO_2 ranging between 500 ppmv and ~200 ppmv (Super et al., 2018), lower Andes (Garzione et al., 2008), open seaways (including east-Tethys and Central American Seaway, hereafter CAS), and reduced icesheets, all of these potentially capable of altering the ITCZ position.

Most modeling studies, for example, Sentman et al. (2018) and see Sepulchre et al. (2014) for a synthesis, show that the closure of CAS induces a strengthening of the Atlantic meridional overturning circulation (AMOC) associated with higher sea surface temperatures in the northern hemisphere and a slight northward shift of the ITCZ (Schneider et al., 2014). Figure 9a shows how the Guajira Peninsula is expected to be even drier than today with an early Miocene-like open CAS, at odds with the empirical records presented earlier showing greater precipitation during the Miocene. Furthermore, numerical experiments with lower Andes (Figure 9b) (Poulsen et al., 2010; Sepulchre et al., 2010) show that the topography did not alter the rainfall patterns over northern South America strongly enough to explain the recorded aridification of La Guajira region.

Quaternary records of precipitation changes in the tropics have long been interpreted as representing a displacement of the ITCZ latitudinal position, in response to latitudinal surface temperature gradients (e.g., Escobar et al., 2012). The ITCZ would expand towards the warmer hemisphere, for example, northward during the mid-Holocene when boreal summer insolation produces north Atlantic warming, or southward during Heinrich events. However, numerical experiments reveal a more complex behavior of the ITCZ. Using reconstructions of SSTs gradients for the Quaternary and its linear relationship with ITCZ latitudinal position obtained from preindustrial and past climate simulations with >20 models, McGee et al. (2014) showed that the maximal latitudinal displacement of the ITCZ as a response to Quaternary abrupt temperature changes would not be higher than one latitudinal degree. This was later explained by the ability of the wind-driven ocean circulation to damp the ITCZ latitudinal displacement (Green & Marshall, 2017). In line with these results, numerical simulations for the mid-Pliocene warm period show neither significant latitudinal displacement of the ITCZ over South America nor increase in precipitation over Guajira (Li et al., 2020; Tan et al., 2020).

Several numerical climate simulations have been carried out for the Miocene. The simulated precipitation response to Miocene boundary conditions is particularly varied for tropical regions, depending on the model used (Henrot et al., 2017). Specifically, atmosphere-only (i.e., with forced SSTs) simulations depict stronger shifts in ITCZ than fully-coupled simulations, as the damping feedback from the ocean mentioned earlier is not accounted for (Lunt et al., 2008). For the middle Miocene over the Guajira region, simulations carried out with CESM1 (Goldner et al., 2014), MPI-ESM (Krapp & Jungclaus, 2011), and Planet Simulator (Henrot et al., 2010) depict drier conditions than the pre-industrial, whereas FOAM-LMDZ (Hamon et al., 2012) and CCSM3 (Herold et al., 2012) simulate slightly wetter conditions, but with values far lower than our reconstructions for the Miocene. In turn, all the models (Goldner et al., 2014; Hamon et al., 2012; Herold et al., 2012; Krapp & Jungclaus, 2011) summarized in Henrot et al. (2017) simulate either a tropical deciduous forest/woodland savanna or a tropical grassland or savanna, but never a wet forest with MAP values around 2,000 mm such as the one predicted here based on palynological data.

Here we compare the most recent Miocene simulation run with CESM 1.0.5 (Zhou et al., 2018) with our reconstructed values of precipitation and temperature. This simulation provides a ~1,000 mm annual rainfall over northeastern South America, with continental surface temperature averaging 28.9°C (Figure 10), a climatic envelope still too warm and too dry when compared with reconstructions. Although the vegetation is prescribed mostly as a tropical rainforest over the region, continental recycling is not sufficient to feed convection and enhance precipitation, possibly as a result of vegetation self-limitation transpiration at high pCO2. Further investigations will also require analysis of the atmospheric dynamics of this simulation to quantify moisture convergence over the Guajira region.

5. Conclusions

Our biostratigraphic analysis may solve a long-standing question about the stratigraphic position of the Oligocene/Miocene boundary in the Cocinetas basin as well as the age of the Siamana Formation and the lower Uitpa Formation. Our results indicate that the top of the Siamana Formation is late Chattian (late Oligocene), that the Uitpa Formation extends from the latest Oligocene (~24.2 Ma) to the early Burdigalian (~19.4 Ma), and that the lower Jimol Formation is Burdigalian (~19.4–17.3 Ma).

The modern vegetation of the Cocinetas Basin is dominated by xerophytic shrubland, which, together with desert occupies more than 90% of the region. The dominance of this type of vegetation is not an effect of early Spanish colonization as historical records indicate that this vegetation was predominant at the time of arrival of the first Europeans to the region. The palynological record of Holocene/modern sediment samples is a good proxy for the present vegetation of the region, yet when compared with the early Miocene palynological record, there is a stark contrast, as the Miocene is dominated by rainforest taxa. This major difference is also seen in the mean annual precipitation, which is ~2,000 mm for the early Miocene, within the envelope of a tropical rainforest. The vertebrate record of the late Neogene of both the Cocinetas and Falcon Basins, although still lacking fossil corroborating plant evidence, suggests that aridity has been a feature only over the past ~3 million years. When and how this change occurred is still a matter of future studies.

Understanding why most Miocene climate simulations fail to reproduce the reconstructed climate conditions over La Guajira is crucial for understanding how the regional climate was driven at the time. First, the present-day atmospheric dynamics over the region together with the sensitivity experiments for the Quaternary indicate that the ITCZ migration alone is unlikely to explain the differences between the Miocene and the present-day climate. Rather, one should explore (i) how moisture convergence patterns and CCLJ are altered during the Miocene, (ii) how the ealier-mentioned subsidence over the Guajira Peninsula is represented in ESMs, and (iii) how moisture convergence behaves with Miocene boundary conditions. A second point is that the Guajira Peninsula is, at the scale of typical climate model resolution, a small region with heterogenous surface conditions. Refining the boundary conditions, including the vegetation and paleotopograpy, together with the use of higher resolution models, could help better represent the Miocene climate of this region. Lastly, constraining the Miocene SSTs of the Caribbean, especially regarding the presence or not of the Guajira upwelling, would help clarify the ocean-atmosphere interactions in this region. The currently under-development modeling intercomparison project for the Miocene ("MioMIP") will help provide such constraints and, we hope, solve the Guajira Miocene climate conundrum.

Data Availability Statement

All data and model outputs analyzed in this study are available open access as NetCDF files on the Zenodo repository, DOI: https://doi.org/10.5281/zenodo.4075108 (https://zenodo.org/record/4075108). Figures 9 and 10 were done using NOAA pyferret within Jupyter notebooks, thanks to the ferretmagic add on developed at LSCE by Patrick Brockmann. Ferret is a product of NOAA's Pacific Marine Environmental Laboratory. (Information is available at http://ferret.pmel.noaa.gov/Ferret [last access: 1 June 2020; NOAA's Pacific Marine Environmental Laboratory, 2020]), distributed under the Open Source Definition. The Jupyter notebook is an open-source web application. Figures 9 and 10 in this paper were made with perceptually uniform, color-vision-deficiency-friendly scientific color maps, developed and distributed by Fabio Crameri (http://www.fabiocrameri.ch/colourmaps.php), to prevent visual distortion of the data (Crameri, 2018).

Acknowledgments

This research was funded by NSF grant EAR-0957679, the National Geographic Society, the Smithsonian Tropical Research Institute, the Anders Foundation, 1923 Fund, and Gregory D. and Jennifer Walston Johnson. We thank the Colombian National Hydrocarbon Agency for access to the Well A samples. We thank S. Lindström, C. Hoorn, M. Huber, and an anonymous reviewer for their constructive comments.

References

Aguilera, O., Lundberg, J., Birindelli, J., Sabaj Pérez, M., Jaramillo, C., & Sánchez-Villagra, M. R. (2013). Palaeontological evidence for the last temporal occurrence of the ancient western Amazonian river outflow into the Caribbean. *PLoS ONE*, *8*(9), e76202. https://doi.org/10.1371/journal.pone.0076202

Aguilera, O., Moraes-Santos, H., Costa, S., Ohe, F., Jaramillo, C., & Nogueira, A. (2013). Ariid sea catfish from the coeval Pirabas (Northeastern Brazil), Cantaure, Castillo (Northwestern Venezuela) and Castilletes (North Colómbia) formations (Early Miocene), with description of three new species. *Swiss Journal of Palaeontology*, *132*(1), 45–68. https://doi.org/10.1007/s13358-013-0052-4

Amson, E., Carrillo, J. D., & Jaramillo, C. (2016). Neogene sloth assemblages (Mammalia, Pilosa) of the Cocinetas Basin (La Guajira, Colombia): Iimplications for the Great American Biotic Interchange. *Palaeontology*, 1–20. https://doi.org/10.1111/pala.12244

Azevedo, J. A. R., Collevatti, R. G., Jaramillo, C., Søren, F., Strömberg, C. A. E., Guedes, T. B., et al. (2020). On the young savannas in the land of ancient forests. In V. Rull & A. Carnaval (Eds.), *Neotropical diversification: Patterns and processes* (pp. 271–299). Cham, Switzerland: Springer Nature. https://doi.org/10.1007/978-3-030-31167-4_12

Backman, J., Raffi, I., Rio, D., Fornaciari, E., & Pälike, H. (2012). Biozonation and biochronology of Miocene through Pleistocene calcareous nannofossils from low and middle latitudes. *Newsletters on Stratigraphy*, *45*(3), 221–244. https://doi.org/10.1127/0078-0421/2012/0022

Backman, J., & Shackleton, N. J. (1983). Quantitative biochronology of Pliocene and early Pleistocene calcareous nannofossils from the Atlantic, Indian and Pacific oceans. *Marine Micropaleontology*, *8*(2), 141–170. https://doi.org/10.1016/0377-8398(83)90009-9

Barrera, E. (2000). *Mestizaje, comercio y resistencia: La Guajira durante la segunda mitad del siglo XVIII*. Bogotá, Colombia: ICAHN.

Braconnot, P., Otto-Bliesner, B., Harrison, S., Joussaume, S., Peterchmitt, J. Y., Abe-Ouchi, A., et al. (2007). Results of PMIP2 coupled simulations of the mid-Holocene and Last Glacial Maximum—Part 2: Feedbacks with emphasis on the location of the ITCZ and mid- and high latitudes heat budget. *Climate of the Past*, *3*(2), 279–296. https://doi.org/10.5194/cp-3-279-2007

Breiman, L. (2001). Random forests. *Machine Learning*, *45*(1), 5–32. https://doi.org/10.1023/A:1010933404324

Bürgi, M., Hersperger, A. M., & Schneeberger, N. (2004). Driving forces of landscape change—Current and new directions. *Landscape Ecology*, *19*(8), 857–868. https://doi.org/10.1007/s10980-004-0245-8

Bush, M. B., & Weng, C. (2007). Introducing a new (freeware) tool for palynology. *Journal of Biogeography*, *34*(3), 377–380. https://doi.org/10.1111/j.1365-2699.2006.01645.x

Butzer, K. W., & Butzert, E. K. (1997). The 'natural' vegetation of the mexican Bajío: Archival documentation of a 16th century savanna environment. *Science*, *43–44*(97), 161–172. https://doi.org/10.1016/s1040-6182(97)00032-3

Cadena, E., & Jaramillo, C. (2015a). Early to middle Miocene turtles from the northernmost tip of South America: Giant testudinids, chelids, and podocnemidids from the Castilletes Formation, Colombia. *Ameghiniana*, *52*(2), 188–203. https://doi.org/10.5710/AMGH.10.11.2014.2835

Cadena, E., & Jaramillo, C. (2015b). The first fossil skull of Chelus (Pleurodira: Chelidae; Matamata genus turtles) from the middle Miocene of Colombia. *Palaeontologia Electronica*, *18.2*(32A), 1–10. https://doi.org/10.26879/545

Carrillo, J. D., Amson, E., Jaramillo, C., Sanchez, R., Quiroz, L., Cuartas, C., & Sanchez-Villagra, M. (2018). The Neogene record of northern South American native ungulates. *Smithsonian Contributions to Paleobiology*, *101*(101), 1–67. https://doi.org/10.5479/si.1943-6688.101

Carrillo-Briceño, J., Argyriou, T., Zapata, V., Kindlimann, R., & Jaramillo, C. (2016). A new Early Miocene (Aquitanian) Elasmobranchi assemblage from the Guajira Peninsula, Colombia. *Ameghiniana*, *53*(2), 77–99. https://doi.org/10.5710/AMGH.26.10.2015.2931

Colinvaux, P., Oliveira, P. E. D., & Moreno, J. E. (1999). *Amazon pollen manual and atlas*. Amsterdam: Hardwood Academic Publishers.

Crameri, F. (2018). Geodynamic diagnostics, scientific visualisation and StagLab 3.0. *Geoscientific Model Development*, *11*(6), 2541–2562. https://doi.org/10.5194/gmd-11-2541-2018

Dale, B. (1976). Cyst formation, sedimentation, and preservation: Factors affecting dinoflagellate assemblages in recent sediments from Trondheimsfjord, Norway. *Review of Palaeobotany and Palynology*, *22*(1), 39–60. https://doi.org/10.1016/0034-6667(76)90010-5

De Verteuil, L., & Norris, G. (1992). Miocene protoperidiniacean dinoflagellate cysts from the Maryland and Virginia coastal plain. In M. J. Head & J. H. Wrenn (Eds.), *Neogene and Quaternary dinoflagellate cysts and acritarchs* (pp. 391–430). Dallas, TX: American Asociation of Stratigraphic Palynologists Foundation.

Dee, D. P., Uppala, S. M., Simmons, A. J., Berrisford, P., Poli, P., Kobayashi, S., et al. (2011). The ERA-Interim reanalysis: Configuration and performance of the data assimilation system. *Quarterly Journal of the Royal Meteorological Society*, *137*(656), 553–597. https://doi.org/10.1002/qj.828

Endfield, G. H., & O'Hara, S. L. (1999). Perception or deception? Land degradation in Post-Conquest Michoácan, west central México. *Land Degradation and Development*, *10*(4), 383–398. https://doi.org/10.1002/(SICI)1099-145X(199907/08)10:4<383::AID-LDR359>3.0.CO;2-7

Escobar, J., Hodell, D. A., Brenner, M., Curtis, J. H., Gilli, A., Mueller, A. D., et al. (2012). A 43-ka record of paleoenvironmental change in the Central American lowlands inferred from stable isotopes of lacustrine ostracods. *Quaternary Science Reviews*, *37*, 92–104. https://doi.org/10.1016/j.quascirev.2012.01.020

Etter, A., McAlpine, C., Wilson, K., Phinn, S., & Possingham, H. (2006). Regional patterns of agricultural land use and deforestation in Colombia. *Agriculture, Ecosystems and Environment*, *114*(2–4), 369–386. https://doi.org/10.1016/j.agee.2005.11.013

Fatela, F., & Taborda, R. (2002). Confidence limits of species proportions in microfossil assemblages. *Marine Micropaleontology*, *45*(2), 169–174. https://doi.org/10.1016/S0377-8398(02)00021-X

Florez, P., Zapata-Ramirez, P., & Klaus, J. S. (2018a). Early Miocene shallow-water corals from La 1 Guajira, Colombia: Part I, Acroporidae–Montastraeidae. *Journal of Paleontology*, *93*, 1–24. https://doi.org/10.1017/jpa.2018.45

Florez, P., Zapata-Ramirez, P., & Klaus, J. S. (2018b). Early Miocene shallow-water corals from La Guajira, Colombia: Part II, Mussidae–Siderastreidae and Milleporidae. *Journal of Paleontology*, *93*, 1–21. https://doi.org/10.1017/jpa.2018.90

Forasiepi, A. M., Soibelzon, L. H., Suarez, C., Sánchez, R., Quiroz, L. I., Jaramillo, C., & Sanchez-Villagra, M. R. (2014). Carnivorans at the Great American Biotic Interchange: New discoveries from the northern Neotropics. *Naturwissenschaften*, *101*(11), 965–974. https://doi.org/10.1007/s00114-014-1237-4

Gamble, D. W., & Curtis, S. (2008). Caribbean precipitation: Review, model and prospect. *Progress in Physical Geography: Earth and Environment*, *32*(3), 265–276. https://doi.org/10.1177/0309133308096027

García-Martínez, I. M., & Bollasina, M. A. (2020). Sub-monthly evolution of the Caribbean low-level jet and its relationship with regional precipitation and atmospheric circulation. *Climate Dynamics*, *54*(9–10), 4423–4440. https://doi.org/10.1007/s00382-020-05237-y

Garzione, C. N., Hoke, G. D., Libarkin, J. C., Withers, S., MacFadden, B. J., Eiler, J., et al. (2008). Rise of the Andes. *Science*, *320*(5881), 1304–1307. https://doi.org/10.1126/science.1148615

Germeraad, J. H., Hopping, C. A., & Muller, J. (1968). Palynology of Tertiary sediments from tropical areas. *Review of Palaeobotany and Palynology*, *6*(3–4), 189–348. https://doi.org/10.1016/0034-6667(68)90051-1

Goldner, A., Herold, N., & Huber, M. (2014). The challenge of simulating the warmth of the mid-Miocene climatic optimum in CESM1. *Climate of the Past*, *10*(2), 523–536. https://doi.org/10.5194/cp-10-523-2014

Green, B., & Marshall, J. (2017). Coupling of trade winds with ocean circulation damps ITCZ shifts. *Journal of Climate*, *30*(12), 4395–4411. https://doi.org/10.1175/JCLI-D-16-0818.1

Hamon, N., Sepulchre, P., Donnadieu, Y., Henrot, A.-J., François, L., Jaeger, J.-J., & Ramstein, G. (2012). Growth of subtropical forests in Miocene Europe: The roles of carbon dioxide and Antarctic ice volume. *Geology*, *40*(6), 567–570. https://doi.org/10.1130/G32990.1

Hendy, A. J. W., Jones, D. S., Moreno, F., Zapata, V., & Jaramillo, C. (2015). Neogene molluscs, shallow-marine paleoenvironments and chronostratigraphy of the Guajira Peninsula, Colombia. *Swiss Journal of Palaeontology*, *134*(1), 45–75. https://doi.org/10.1007/s13358-015-0074-1

Henrot, A.-J., François, L., Favre, E., Butzin, M., Ouberdous, M., & Munhoven, G. (2010). Effects of CO_2, continental distribution, topography and vegetation changes on the climate at the Middle Miocene: A model study. *Climate of the Past*, *6*(5), 675–694. https://doi.org/10.5194/cp-6-675-2010

Henrot, A. J., Utescher, T., Erdei, B., Dury, M., Hamon, N., Ramstein, G., et al. (2017). Middle Miocene climate and vegetation models and their validation with proxy data. *Paleogeography, Paleoeclimatology, Paleoecology*, *467*, 95–119. https://doi.org/10.1016/j.palaeo.2016.05.026

Herold, N., Huber, M., Müller, R., & Seton, M. (2012). Modeling the Miocene climatic optimum: Ocean circulation. *Paleoceanography*, *27*, PA1209. https://doi.org/10.1029/2010pa002041

Hijmans, R. J., Cameron, S. E., Parra, J. L., Jones, P. G., & Jarvis, A. (2005). Very high resolution interpolated climate surfaces for global land areas. *International Journal of Climatology*, *25*(15), 1965–1978. https://doi.org/10.1002/joc.1276

Hofmann, C. (2002). Pollen distribution in sub-recent sedimentary environments of the Orinoco Delta (Venezuela)—An actuo-palaeobotanical study. *Review of Palaeobotany and Palynology*, *119*(3–4), 191–217. https://doi.org/10.1016/S0034-6667(01)00141-5

Hoorn, C. (1994). An environmental reconstruction of the palaeo-Amazon River system (middle-late Miocene, NW Amazonia). *Palaeogeography, Palaeoclimatology, Palaeoecology*, *112*(3–4), 187–238. https://doi.org/10.1016/0031-0182(94)90074-4

Hoyos, I., Dominguez, F., Cañón-Barriga, J., Martínez, J. A., Nieto, R., Gimeno, L., & Dirmeyer, P. A. (2018). Moisture origin and transport processes in Colombia, northern South America. *Climate Dynamics*, *50*(3–4), 971–990. https://doi.org/10.1007/s00382-017-3653-6

Instituto de Hidrología, M. y. E. A., Instituto Alexander von, H., Instituto Geográfico Agustín, C., Instituto de Investigaciones Marinas y Costeras "José Benito Vives de, A., & Ministerio de Ambiente y Desarrollo, S (2017). *Mapa de Ecosistemas Continentales, Costeros y Marinos de Colombia (MEC) [Map] V. 2.1, escala 1:100.000*. Bogotá: Instituto de Hidrología, Meteorología y Estudios Ambientales.

Jaramillo, C. (2019). 140 million years of tropical biome evolution. In J. Gomez & A. O. Pinilla-Chacon (Eds.), *The geology of Colombia, Volume 2 Mesozoic* (Vol. 2, pp. 1–28). Bogotá: Servicio Geológico Colombiano. https://doi.org/10.32685/pub.esp.36.2019.06

Jaramillo, C., & Cardenas, A. (2013). Global warming and neotropical rainforests: A historical perspective. *Annual Review of Earth and Planetary Sciences*, *41*(1), 741–766. https://doi.org/10.1146/annurev-earth-042711-105403

Jaramillo, C., Moreno, E., Ramirez, V., da Silva, S., Barrera, A., Adhara, B., et al. (2014). Palynological record of the last 20 million years in Panama. In W. D. Stevens, O. M. Montiel, P. Raven (Eds.), *Paleobotany and biogeography: A Festschrift for Alan Graham in his 80th year* (Vol. 128, pp. 134–253). St Louis, Missouri: Missouri Botanical Garden Press.

Jaramillo, C., Moreno, F., Hendy, F., Sanchez-Villagra, M., & Marty, D. (2015). Preface: La Guajira Colombia: A new window into the Cenozoic neotropical biodiversity and the Great American Biotic Interchange. *Swiss Journal of Palaeontology*, *134*, 1–4. https://doi.org/10.1007/s13358-015-0075-0

Jaramillo, C., Romero, I., D'Apolito, C., Bayona, G., Duarte, E., Louwye, S., et al. (2017). Miocene flooding events of western Amazonia. *Science Advances*, *3*(5), e1601693. https://doi.org/10.1126/sciadv.1601693

Jaramillo, C., & Rueda, M. (2019). *A morphological electronic database of Cretaceous-Tertiary and extant pollen and spores from Northern South America, v. 2019*. Panamá City, Panamá: Smithsonian Tropical Research Institute.

Jaramillo, C., Rueda, M., & Torres, V. (2011). A palynological zonation for the Cenozoic of the Llanos Foothills of Colombia. *Palynology*, *35*(1), 46–84. https://doi.org/10.1080/01916122.2010.515069

Johnson, K. G., Sanchez-Villagra, M., & Aguilera, O. A. (2009). The Oligocene-Miocene transition on coral reefs in the Falcon Basin (NW Venezuela). *PALAIOS*, *24*(1), 59–69. https://doi.org/10.2110/palo.2008.p08-004r

Kennett, J. P., & Srinivasan, M. S. (1983). *Neogene planktonic foraminifera, a phylogenetic atlas*. Stroudsburg, Pennsylvania: Hutchinson Ross.

Krapp, M., & Jungclaus, J. (2011). The Middle Miocene climate as modelled in an atmosphere–ocean–biosphere model. *Climate of the Past*, *7*(4), 1169–1188. https://doi.org/10.5194/cp-7-1169-2011

Li, X., Guo, C., Zhang, Z., Otterå, O. H., & Zhang, R. (2020). PlioMIP2 simulations with NorESM-L and NorESM1-F. *Climate of the Past*, *16*(1), 183–197. https://doi.org/10.5194/cp-16-183-2020

Liaw, A., & Wiener, M. (2002). Classification and regression by randomForest. *R News*, *2*(3), 18–22. https://doi.org/10.1023/A:1010933404324

Liu, X., Battisti, D. S., & Donohoe, A. (2017). Tropical precipitation and cross-equatorial ocean heat transport during the mid-Holocene. *Journal of Climate*, *30*(10), 3529–3547. https://doi.org/10.1175/JCLI-D-16-0502.1

Lorente, M. A. (1986). *Palynology and palynofacies of the Upper Tertiary in Venezuela*. Berlin: J. Cramer.

Lunt, D. J., Flecker, R., Valdes, P. J., Salzmann, U., Gladstone, R., & Haywood, A. M. (2008). A methodology for targeting palaeo proxy data acquisition: A case study for the terrestrial late Miocene. *Earth and Planetary Science Letters*, *271*(1–4), 53–62. https://doi.org/10.1016/j.epsl.2008.03.035

Maitner, B. S., Boyle, B., Casler, N., Condit, R., Donoghue, J. II, Durán, S. M., et al. (2018). The bien r package: A tool to access the Botanical Information and Ecology Network (BIEN) database. *Methods in Ecology and Evolution*, *9*(2), 373–379. https://doi.org/10.1111/2041-210x.12861

Martelo, M. T. (2003). *La precipitacion en Venezuela y su relacion con el sistema climatico*. Caracas: Direccion de Hidrologia, Metereologia y Oceanografia-Direccion General del Cuencas Hidrograficas.

Martini, E. (1971). Standard Tertiary and Quaternary calcareous nannoplankton zonation. In A. Farinacci (Ed.), *Proceedings 2nd International Conference Planktonic Microfossils Roma* (pp. 739–785). Rome: Tecnoscienza.

Mass, M., & Burgos, A. (2011). Water dynamics at the ecosystem level in seasonally dry tropical forests. In R. Dirzo, H. S. Young, H. A. Mooney, G. Ceballos (Eds.), *Seasonally dry tropical forests* (pp. 141–156). Washington, DC: Island Press. https://doi.org/10.5822/978-1-61091-021-7_9

Matteucci, S. (1987). The vegetation of Falcón State, Venezuela. *Vegetatio*, *70*(2), 67–91. https://doi.org/10.1007/BF00041474

Matteucci, S. D., Colma, A., & Pla, L. (1982). Desertification maps of Falcon State, Venezuela. *Environmental Conservation*, *9*(3), 217–224. https://doi.org/10.1017/S0376892900020427

McGee, D., Donohoe, A., Marshall, J., & Ferreira, D. (2014). Changes in ITCZ location and cross-equatorial heat transport at the Last Glacial Maximum, Heinrich Stadial 1, and the mid-Holocene. *Earth and Planetary Science Letters*, *390*, 69–79. https://doi.org/10.1016/j.epsl.2013.12.043

Medina, E., Cram, W. J., Lee, H. S. J., Lüttge, U., Popp, M., Smith, J. A. C., & Diaz, M. (1989). Ecophysiology of xerophytic and halophytic vegetation of a coastal alluvial plain in northern Venezuela. *New Phytologist*, *111*(2), 233–243. https://doi.org/10.1111/j.1469-8137.1989.tb00688.x

Montes, C., Rodriguez-Corcho, A. F., Bayona, G., Hoyos, N., Zapata, S., & Cardona, A. (2019a). Continental margin response to multiple arc-continent collisions: The northern Andes-Caribbean margin. *Earth Science Reviews*, *198*, 102903. https://doi.org/10.1016/j.earscirev.2019.102903

Montes, C., Rodriguez-Corcho, A. F., Bayona, G., Hoyos, N., Zapata, S., & Cardona, A. (2019b). *GPlates Dataset for the Tectonic Reconstruction of the Northern Andes-Caribbean Margin. Data In Brief* (Vol. 25, p. 104398). Amsterdam: Elsevier. https://doi.org/10.1016/j.dib.2019.104398

Moreno, E., Vergara, D., & Jaramillo, C. (2014). Las colecciones palinológicas del Instituo Smithsonian de Investigaciones Tropicales (STRI), Panamá. *Boletín de la Asociación LAtinoamericana de Paleobotánica y Palinología*, *14*, 207–222.

Moreno, J. F., Hendy, A. J. W., Quiroz, L., Hoyos, N., Jones, D. S., Zapata, V., et al. (2015). An overview and revised stratigraphy of Early Miocene-Pliocene deposits in Cocinetas Basin, La Guajira, Colombia. *Swiss Journal of Palaeontology*, *134*(1), 5–43. https://doi.org/10.1007/s13358-015-0071-4

Moreno-Bernal, J. W., Head, J., & Jaramillo, C. (2016). Fossil Crocodilians from the High Guajira Peninsula of Colombia: Neogene faunal change in northernmost South America. *Journal of Vertebrate Paleontology*, *36*(3), e1110586. https://doi.org/10.1080/02724634.2016.1110586

Muller, J. (1959). Palynology of recent Orinoco delta and shelf sediments: Reports of the Orinoco Shelf Expedition; Volume 5. *Micropaleontology*, *5*(1), 1–23. https://doi.org/10.2307/1484153

Muller, J., Di Giacomo, E., & Van Erve, A. (1987). A palynologic zonation for the Cretaceous, Tertiary and Quaternary of Northern South America. In *American Association of Stratigraphic Palynologists Contribution Series* (Vol. 19, pp. 7–76). Dallas, TX: American Association of Stratigraphic Palynologists Foundation.

Navarrete Peláez, M. (2003). La granjería de las perlas del Río de la Hacha: rebelión y resistencia esclava (1570-1615). *Historia Caribe*, *8*, 35–50.

Perez, M., Vallejo-Pareja, M. C., Carrillo, J. D., & Jaramillo, C. (2017). A new Pliocene capybara (Rodentia, Caviidae) from northern South America (Guajira, Colombia), and its implications for the Great American Biotic Interchange. *Journal of Mammalian Evolution*, *24*(1), 111–125. https://doi.org/10.1007/s10914-016-9356-7

Perez-Consuegra, N., Parra, M., Jaramillo, C., Silvestro, D., Echeverri, S., Montes, C., et al. (2018). Provenance analysis of the Pliocene Ware Formation in the Guajira Peninsula, northern Colombia: Paleodrainage implications. *Journal of South American Earth Sciences*, *81*, 66–77. https://doi.org/10.1016/j.jsames.2017.11.002

Polo Acuña, J. (1998). Aspectos Historicos De Riohacha Durante El Periodo Colonial. *Historia Caribe*, *II*(3), 33–48.

Poulsen, C. J., Ehlers, T. A., & Insel, N. (2010). Onset of convective rainfall during gradual Late Miocene rise of the Central Andes. *Science*, *328*(5977), 490–493. https://doi.org/10.1126/science.1185078

Quiroz, L., & Jaramillo, C. (2010). Stratigraphy and sedimentary environments of Miocene shallow to marginal marine deposits in the Urumaco Trough, Falcon Basin, western Venezuela. In M. Sanchez-Villagra, O. Aguilera, A. A. Carlini (Eds.), *Urumaco and Venezuelan palaeontology. The fossil record of the Northern Neotropics* (pp. 153–172). Bloomington, Indiana: Indiana University Press.

R-Development-Core-Team (2019). R: A language and environment for statistical computing. In *R Foundation for Statistical Computing*. Vienna, Austria: R Foundation for Statistical Computing.

Roubik, D. W., & Moreno, J. E. (1991). *Pollen and spores of Barro Colorado Island* (Vol. 36). St. Louis, Missouri: Missouri Botanical Garden.

Sánchez-Villagra, M. R., Aguilera, O. A., Sanchez, R., & Carlini, A. A. (2010). The fossil vertebrate record of Venezuela of the last 65 million years. In M. R. Sánchez-Villagra, O. A. Aguilera, A. A. Carlini (Eds.), *Urumaco and Venezuelan palaeontology. The fossil record of the Northern Neotropics* (pp. 19–51). Bloomington, Indiana: Indiana University Press.

Sarmiento, G. (1975). The dry plant formations of South America and their floristic connections. *Journal of Biogeography*, *2*(4), 233–251. https://doi.org/10.2307/3037998

Schneider, T., Bischoff, T., & Haug, G. H. (2014). Migrations and dynamics of the intertropical convergence zone. *Nature*, *513*(7516), 45–53. https://doi.org/10.1038/nature13636

Scholz, S. R., Petersen, S. V., Escobar, J., Jaramillo, C., Hendy, A. J. W., Allmon, W. D., et al. (2020). Isotope schlerochronology indicates enhanced precipitation seasonality in northern South America (Colombia) during the Mid-Miocene Climatic Optimum. *Geology*, *48*. https://doi.org/10.1130/G47235.47231

Sentman, L. T., Dunne, J. P., Stouffer, R. J., Krasting, J. P., Toggweiler, J. R., & Broccoli, A. J. (2018). The mechanistic role of the central American seaway in a GFDL earth system model. Part 1: Impacts on global ocean mean state and circulation. *Paleoceanography and Paleoclimatology*, *33*(7), 840–859. https://doi.org/10.1029/2018PA003364

Sepulchre, P., Arsouze, T., Donnadieu, Y., Dutay, J.-C., Jaramillo, C., Le Bras, J., et al. (2014). Consequences of shoaling of the Central American Seaway determined from modeling Nd isotope. *Paleoceanography*, *29*(3), 176–189. https://doi.org/10.1002/2013PA002501

Sepulchre, P., Sloan, L. C., & Fluteau, F. (2010). Modelling the response of Amazonian climate to the uplift of the Andean mountain range. In M. C. Hoorn & F. P. Wesselingh (Eds.), *Amazonia, landscape and species evolution: A look into the past* (pp. 211–222). Oxford: Wiley-Blackwell Publishing.

Silva-Caminha, S., Jaramillo, C., & Absy, M. L. (2010). *Neogene palynology of the Solimões Basin, Brazilian Amazonia* (Vol. 283, pp. 1–67). Stuttgart: Palaeontographica Abteilung B.

Silva-Tamayo, J. C., Lara, M. E., Nana Yobo, L., Erdal, Y. D., Sanchez, J., & Zapata-Ramirez, P. A. (2017). Tectonic and environmental factors controlling on the evolution of Oligo-Miocene shallow marine carbonate factories along a tropical SE Circum-Caribbean. *Journal of South American Earth Sciences*, *78*, 213–237. https://doi.org/10.1016/j.jsames.2017.06.008

Soares, E. A., D'Apolito, C., Jaramillo, C., Harrington, G., Caputo, M., Barbosa, R., et al. (2017). Sedimentology and Palynostratigraphy of a Pliocene-Pleistocene (Piacenzian to Gelasian) deposit in the lower Negro River: Implications to the establishment of large rivers in Central Amazonia. *Journal of South American Earth Sciences*, *79*, 215–229. https://doi.org/10.1016/j.jsames.2017.08.008

Suarez, C., Forasiepi, A. M., Goin, F. J., & Jaramillo, C. (2016). Insights into the Neotropics prior to the Great American Biotic Interchange: New evidence of mammalian predators from the Miocene of Northern Colombia. *Journal of Vertebrate Paleontology*, *36*(1), e1029581. https://doi.org/10.1080/02724634.2015.1029581

Super, J. R., Thomas, E., Pagani, P., Huber, M., O'Brien, C., & Hull, P. M. (2018). North Atlantic temperature and PCO_2 coupling in the Early-Middle Miocene. *Geology*, *46*(6), 519–522. https://doi.org/10.1130/G40228.1

Tan, N., Contoux, C., Ramstein, G., Sun, Y., Dumas, C., Sepulchre, P., & Guo, Z. (2020). Modeling a modern-like PCO_2 warm period (marine isotope stage KM5c) with two versions of an Institut Pierre Simon Laplace Atmosphere–Ocean cCoupled General Circulation Model. *Climate of the Past*, *16*(1), 1–16. https://doi.org/10.5194/cp-16-1-2020

Thomas, F. C., & Murney, M. G. (1985). Techniques for extraction of foraminifers and ostracodes from sediments samples. In *Canadian Technical Report of Hydrography and Ocean Sciences* (Vol. 54, pp. 1–24). Dartmouth, Nova Scotia: Canada Department of Fisheries and Oceans.

Tovar, H. (1992). Relaciones y visitas a los Andes (S. XVI). In *Región del Caribe de Colección de Historia de la Biblioteca Nacional* (pp. 1–436). Colcultura e Instituto Colombiano de Cultura Hispánica.

Traverse, A. (2007). *Paleopalynology* (2nd ed.). Dordrecht: Springer. https://doi.org/10.1007/978-1-4020-5610-9

Turner, B. L., & Butzer, K. W. (1992). The Columbian encounter and land-use change. *Environment*, *34*(8). https://doi.org/10.1080/00139157.1992.9931469

Vásquez, S., & Correa, H. (1993). *Los wayuu, entre juya (el que llueve) Mma (la tierra) y el desarrollo urbano regional* (pp. 215–292). Bogotá: Instituto Colombiano de Cultura Hispánica.

Wade, B. S., Pearson, P. N., Berggren, W. A., & Pälike, H. (2011). Review and revision of Cenozoic tropical planktonic foraminiferal biostratigraphy and calibration to the geomagnetic polarity and astronomical time scale. *Earth Science Reviews*, *104*(1–3), 111–142. https://doi.org/10.1016/j.earscirev.2010.09.003

Wade, B. S., Pearson, P. N., Olsson, R. K., Fraass, A. J., Leckie, R. M., & Hemleben, C. (2018). Taxonomy, biostratigraphy, and phylogeny of Oligocene and Lower Miocene Dentoglobigerina and Globoquadrina. In B. S. Wade, R. K. Olsson, P. N. Pearson, B. T. Huber, W. A. Berggren (Eds.), *Atlas of Oligocene planktonic foraminifera* (pp. 331–385). London: Cushman Foundation for Foraminiferal Research Special Publication.

Wand, M., & Jones, M. C. (1994). *Kernel smoothing*. London: Chapman and Hall. https://doi.org/10.1201/b14876

Wang, C. (2007). Variability of the Caribbean low-level jet and its relations to climate. *Climate Dynamics*, *29*(4), 411–422. https://doi.org/10.1007/s00382-007-0243-z

Young, J. P. (1998). Neogene. In P. R. Bown (Ed.), *Calcareous nannofossil biostratigraphy* (pp. 225–265). London: Chapman & Hall. https://doi.org/10.1007/978-94-011-4902-0_8

Young, J. R., Wade, B. S., & Huber, B. T. (2017). *pforams@mikrotax website* http://www.mikrotax.org/pforams

Zhou, H., Helliker, B. R., Huber, M., Dicks, A., & Akçay, E. (2018). C_4 photosynthesis and climate through the lens of optimality. *Proceedings of the National Academy of Sciences*, *115*, 12,057–12,062. https://doi.org/10.1073/pnas.1718988115

References From the Supporting Information

Agnini, C., Fornaciari, E., Raffi, I., Catanzariti, R., Pälike, H., Backman, J., & Rio, D. (2014). Biozonation and biochronology of Paleogene calcareous nannofossils from low and middle latitudes. *Newsletters on Stratigraphy*, *47*(2), 131–181. https://doi.org/10.1127/0078-0421/2014/0042

Archivo_General_da_las_Indias, A. (1744). *Mapa de las barras de la laguna de Maracaibo, de la ensenada que ay entre los dos cabos de Sancta Anna y Chichibacoa, y parte de las costas que desde ellos corren assi al este y vueste, cuyos paizes se reconocerán por sus demonstratibos, y las distancias*. Archivo General da las Indias: Seville.

Aubry, M.-P. (2014). Cenozoic coccolithophores: Discoasterales (CC-B). In *Cenozoic coccolithophores* (pp. 1–431). New York: Micropaleontology Press.

Ballesteros, M. J. (1962). Carta del Obispo de Coro Don Miguel Jerónimo Ballesteros al Rey de España, dándole cuenta de haber tomado posesión de su mitra, y de como encontró su obispado, en 20 de octubre de 1550. In J. Gabaldon Márquez (Ed.), *Descubrimiento y conquista de Venezuela: textos históricos contemporáneos y documentos fundamentales. Tomo 2 Cubagua y la empresa de los Belzares* (pp. 17–41). Academia Nacional de la Historia: Italgráfica.

Becker, L. E., & Dusenbury, A. N. (1958). *Mio-Oligocene (Aquitanian) foraminifera from the Guajira Peninsula, Colombia* (Vol. 4, pp. 1–48). Lawrence, Kansas: Cushman Foundation for Foraminiferal Research, Special Publication.

Bolivar, S. (1972). *Carta de Jamaica*. Mexico City, Mexico: Universidad Autónoma de México.

Bolli, H. M., & Saunders, J. B. (1985). Oligocene to Holocene low latitude planktic foraminifera. In H. M. Bolli, J. B. Saunders, K. Perch-Nielsen (Eds.), *Plankton Stratigraphy* (pp. 155–262). London: Cambridge University Press.

Castellanos, J. d. (1847). *Elegías de Varones Ilustres de Indias*. Rivadeneyra: Imprenta y estereotipía de M.

de Oviedo, F., Valdés, G., de Tudela, P., & Bueso, J. (1959). *Historia general y natural de las Indias*. Madrid: Tomo III. Ediciones Atlas.

Duffield, S. L., & Stein, J. A. (1986). Peridiniacean-dominated dinoflagellate cyst assemblages from the Miocene of the Gulf of Mexico shelf, offshore Louisiana. In *AASP Contribution Series* (Vol. 17, pp. 27–45). Dallas, TX: American Association of Stratigraphic Palynologists Foundation.

Eaton, G. L., Fensome, R. A., Riding, J. B., & Williams, G. L. (2001). Re-evaluation of the status of the dinoflagellate cyst genus Cleistosphaeridium. *Neues Jahrbuch für Geologie und Paläontologie (Abhandlungen)*, *219*(1–2), 171–205. https://doi.org/10.1127/njgpa/219/2001/171

Edwards, L. E., Weems, R. E., Carter, M. W., Spears, D. B., & Powars, D. S. (2018). The significance of dinoflagellates in the Miocene Choptank Formation beneath the Midlothian gravels in the southeastern Virginia Piedmont. *Stratigraphy*, *15*(3), 179–195. https://doi.org/10.29041/strat.15.179-195

Federman, N. d. (1958). *Historia Indiana*. Bogotá: Carco.

Helenes, J., & Cabrera, D. (2003). Oligocene-Miocene palynomorph assemblages from eastern Venezuela. *Palynology*, *27*(1), 5–25. https://doi.org/10.1080/01916122.2003.9989579

Hilgen, F. J., Lourens, L. J., Van Dam, J. A., Beu, A. G., Boyes, A. F., Cooper, R. A., et al. (2012). Chapter 29—The Neogene period. In F. M. Gradstein, J. G. O. D. Schmitz, G. M. Ogg (Eds.), *The geologic time scale* (pp. 923–978). Boston, MA: Elsevier. https://doi.org/10.1016/B978-0-444-59425-9.00029-9

Köthe, A., & Piesker, B. (2007). Stratigraphic distribution of Paleogene and Miocene dinocysts in Germany. In *Revue de Paléobiologie* (Vol. 26, pp. 1–39). Geneva: Muséum d'histoire naturelle de Genève.

Leckie, R. M., Wade, B. S., Pearson, P. N., Fraass, A. J., King, D. J., Olsson, R. K., et al. (2018). Taxonomy, biostratigraphy, and phylogeny of Oligocene and Lower Miocene Paragloborotalia and Parasubbotina. In B. S. Wade, R. K. Olsson, P. N. Pearson, B. T. Huber, W. A. Berggren (Eds.), *Atlas of Oligocene planktonic foraminifera* (pp. 125–179). London: Cushman Foundation for Foraminiferal Research Special Publication.

Lenoir, E. A., & Hart, G. F. (1986). Burdigalian (early Miocene) dinocysts from offshore Louisiana. In *AASP Contribution Series* (Vol. 17, pp. 59–81). Dallas, TX: American Association of Stratigraphic Palynologists Foundation.

Lockwood, J. P. (1965). *Geology of the Serrania de Jarara Area Guajira Peninsula*. Princeton: Colombia Princeton University.

López de Velasco, J. (1964). Corografía de la Gobernación de Venezuela y Nueva Andalucía, 1571–1574, por Juan Lopez de Velasco. In A. Arellano Moreno (Ed.), *Relaciones Geográficas de Venezuela* (pp. 173–199). Caracas: Italgráfica, Academia Nacional de la Historia.

Louwye, S., Foubert, A., Mertens, K., & Van Rooij, D. (2008). Integrated stratigraphy and palaeoecology of the Lower and Middle Miocene of the Porcupine Basin. *Geological Magazine*, *145*(3), 321–344. https://doi.org/10.1017/S0016756807004244

MADS (2015). *Mapa de ecosistemas continentales, costeros y marinos de Colombia version 1.0. Escala 1:100,000. Bogota, MADS_IDEAM_IAvH_INVEMAR_IIAP_SINCHI_PNN_IGAC*. Bogotá: Instituto de Hidrología, Meteorología y Estudios Ambientales.

Martin, E. (1962). Relación de la expedición de Ambrosio Alfinger. 9 de Junio de 1531, hasta el 2 de noviembre de 1533. Escrita por Esteban Martin, Maestre de campo de Ambrosio Alfinger. In A. Arellano Moreno (Ed.), *Descubrimiento y conquista de Venezuela: textos históricos contemporáneos y documentos fundamentales. Vol. 2 Cubagua y la empresa de los Belzares* (pp. 254–270). Caracas: Italgráfica, Academia Nacional de la Historia.

Navarrete, R. d., & Barbudo, A. (1964). Relación de las provincias y naciones de los indios aruacas, hecha por Rodrigo de Navarrete y memoria de Antonio Barbudo sobre los territorios costaneros (1570–1575). In A. Arellano Moreno (Ed.), *Relaciones Geográficas de Venezuela* (pp. 81–96). Caracas: Italgráfica, Academia Nacional de la Historia.

Naveros, A. (1962). Carta de Antonio de Naveros y Alonso Vásquez de Acuña al Rey. El primero hace relación de la primera entrada de Federman; hay muchos otros datos sobre este último y sobre Ambrosio de Alfinger. In A. N. Historia (Ed.), *Descubrimiento y conquista de Venezuela: textos históricos contemporáneos y documentos fundamentales. Tomo 2 Cubagua y la empresa de los Belzares* (pp. 274–319). Caracas: Italgráfica Academia Nacional de la Historia.

Ocampo, M. J. D., & Montalvo de Jarama, M. (1956). Nueva Umbría. In *Conquista y colonización de este reino en 1518* (pp. 1–255). Madrid: Sociedad española de Librería.

Olsson, R. K., Hemleben, C., Coxall, H. K., & Wade, B. S. (2018). Taxonomy, biostratigraphy, and phylogeny of Oligocene Ciperoella. In B. S. Wade, R. K. Olsson, P. N. Pearson, B. T. Huber, & W. A. Berggren (Eds.), *Atlas of Oligocene Planktonic Foraminifera* (pp. 215–231). London: Cushman Foundation for Foraminiferal Research Special Publication.

Oviedo, G. (1986). *Historia general y natural de las indias: La provincia de Venezuela*. Caracas: Fundacion de Promocion Cultural de Venezuela.

Perch-Nielsen, K. (1985). Cenozoic calcareous nannofossils. In H. H. Bolli, J. B. Saunders, K. Perch-Nielsen (Eds.), *Plankton Stratigraphy* (pp. 427–555). Cambridge: Cambridge University Press.

Perez-Consuegra, N., Gongora, D. E., Herrera, F., Jaramillo, C., Montes, C., Cuervo-Gomez, L., et al. (2018). New records of Humiriaceae fossil fruits from the Oligocene and Early Miocene of the western Azuero Peninsula, Panamá. *Boletín de la Sociedad Geológica Méxicana*, *70*(1), 223–239. https://doi.org/10.18268/BSGM2018v70n1a13

Rollins, J. F. (1965). *Stratigraphy and structure of the Goajira Peninsula, nortwestern Venezuela and northeastern Colombia* (Vol. 30, pp. 1–102). Lincoln, Nebraska: University of Nebraska Studies: New Series.

Soliman, A., Ćorić, S., Head, M. J., Piller, W. E., & El Beialy, S. Y. (2012). Lower and Middle Miocene biostratigraphy, Gulf of Suez, Egypt based on dinoflagellate cysts and calcareous nannofossils. *Palynology*, *36*(1), 38–79. https://doi.org/10.1080/01916122.2011.633632

Spezzaferri, S., Coxall, H. K., Olsson, R. K., & Hemleben, C. (2018). Taxonomy, biostratigraphy, and phylogeny of Oligocene Globigerina, Globigerinella, and Quiltyella n. gen. In B. S. Wade, R. K. Olsson, P. N. Pearson, B. T. Huber, W. A. Berggren (Eds.), *Atlas of Oligocene planktonic foraminifera* (pp. 179–215). London: Cushman Foundation for Foraminiferal Research Special Publication.

Tolosa, J. (1964). Relaciones Geograficas de Venezuela. In A. Arellano Moreno (Ed.), *Relaciones Geográficas de Venezuela* (pp. 1–578). Caracas: Italgráfica, Academia Nacional de la Historia.

Varol, O. (1998). Palaeogene. In P. R. Bown (Ed.), *Calcareous nannofossil biostratigraphy* (pp. 200–224). London: Chapman & Hall. https://doi.org/10.1007/978-94-011-4902-0_7

Williams, G. L., Brinkhuis, H., Pearce, M. A., Fensome, R. A., & Weegink, J. W. (2004). Southern Ocean and global dinoflagellate cyst events compared: Index events for the Late Cretaceous–Neogene. In *Proceedings of the Ocean Drilling Program, Scientific Results* (Vol. 189, pp. 1–98). College Station, TX: Ocean Drilling Program.